2019-08-20

Ice Nucleation: Sulfate and Its Influence in Arctic and Rural and Urban NW Continental Precipitation

Derksen, Mark

UNIVERSITY OF CALGARY

Ice Nucleation: Sulfate and Its Influence in Arctic and Rural and Urban NW Continental Precipitation

by

Mark Derksen

A THESIS

SUBMITTED TO THE FACULTY OF GRADUATE STUDIES

IN PARTIAL FUFULMENT OF THE REQUIREMENTS FOR THE

DEGREE OF MASTER OF SCIENCE

GRADUATE PROGRAM IN PHYSICS AND ASTRONOMY

CALGARY, ALBERTA

AUGUST, 2019

Abstract

With the growth of urban centers and decline of natural ecosystems, the increasing presence of aerosol particles has the potential to have major impacts on climate. This study assessed the ice nucleation characteristics of anthropogenic and organic/biogenic sulfate sources in precipitation samples from the Arctic, Kananaskis (rural continental), and Calgary (Urban continental). Samples were analyzed using droplet freezing technique, isotopic analysis, and anion/cation measurements. Comparisons between deposition-based precipitation sampler and passive fog/rain sampler yielded no significant differences in ice nucleation characteristics. Arctic fog samples had distinct ice nucleating particle characteristics compared to rain and dry deposition samples. A 32% increase in the influence of biogenic matter was apparent in 2016 Arctic samples relative to 2014 samples. The influence of a continental biogenic and/or organic material was apparent in the ice nucleating characteristics of both rural and urban continental samples. Snow samples exhibited the greatest biogenic influence, followed by rain samples, and then dry deposition samples.

Acknowledgements

This thesis would not have been possible with the help of so many people, and I am very grateful to you all!

First and foremost, I would like to thank my supervisor Dr. Ann-Lise Norman for the extensive guidance, mentorship, motivation, and encouragement. This project provided me with amazing opportunities to grow and learn as a researcher. Thank you to Dr. Mike Wieser and Dr. David Hobill for the invaluable feedback, and lending your expertise, time, and support.

Thank you to my lab colleagues Roghayeh Ghahremaninezhadgharelar, Chenqi Ge, and Neda Amiri. You were always happy to lend a hand or answer my questions. Thank you to Farzin Malekani for the technical assistance in laboratory sample analysis. Thank you to my longtime mentor and friend Dr. Trent Hoover, for your endless advice and support.

I would like to dedicate a special thanks towards my friends and family, who were always supportive and encouraging during my project.

Table of Contents

List of Tables

List of Figures and Illustrations

List of Abbreviations

AVOS	Automated Voluntary Observation System
BC	Black Carbon
CCN Cloud Condensation Nuclei	Cloud Condensation Nuclei
CDFC	Continuous Flow Thermal Gradient Diffusion Chambers
CF-IRMS	Continuous-flow isotope ratio mass spectrometry
CLAW	Charlson Lovelock Andreae Warren Hypothesis
DFT	Droplet Freezing Technique
DMS	Dimethyl Sulfide
DMSP	Dimethylsulfoniopropionate
ESRL	Earth System Research Laboratory
GEOS-Chem	Goddard Earth Observing System Chemistry Model
GHG	Greenhouse Gas
HYSPLIT	Hybrid Single Particle Lagrangian Integrated Trajectory Model
IN Ice Nuclei	Ice Nuclei
INP/L Ice Nucleating Particles / Liter	Ice Nucleating Particles / L
IPCC	Intergovernmental Panel on Climate Change
MSA	Methane Sulfonic Aced
NETCARE	Network on Climate and Aerosols: Addressing Key Uncertainties in Remote Canadian Environments
NOAA	National Oceanic and Atmospheric Administration
NSS	Non Sea Salt
SS	Sea Salt
STB	An isotope standard: identical carbonatite sample powders analyzed at Stony Brook
VCDT	Vienna-Canyon Diablo Troilite

Chapter One: Introduction

1.1 Atmospheric Aerosol Impacts and Sulfate Influences

GHG (greenhouse gas) emissions over the past century have been steadily increasing as a result of growing fossil fuel usage. This has contributed to increases in average surface temperatures, global sea-level rise, and fluctuations of global and regional radiation budgets (NOAA/ESRL Global Monitoring Division; Maxwell, 1992; Koivurova., 2017).

One major factor affecting the atmospheric radiation budget is the presence of particulate matter in the form of aerosol particles (Rosenfeld, 2006). Aerosol particles are suspensions of fine solid particles or liquid droplets originating from both anthropogenic and natural sources. With the growth of urban centers and decline of natural ecosystems, the increasing presence of these ubiquitous particles have the potential to have major impacts on climate (Ibald-Mulli et al., 2002).

Most aerosol particles originate from natural sources like volcanoes, forest fires, oceanic, and desert sources, while a smaller portion (~10%) result from anthropogenic influences like fossil fuel combustion and biomass burning (Brimblecombe, 2013). A significant portion of atmospheric aerosols are sulfates, which result from processes that produce sulfurous gases like Sulfur Dioxide, or other organosulfur compounds like Dimethyl Sulfide (DMS). As surface temperatures rise, and solar radiation increases, sources of marine sulfate (such as algae blooms) are provided with more hospitable conditions for growth.

The purpose of this study is to investigate the influence of sulfate in ice nucleation processes in the Arctic, as well as mid-latitude Rural, and Urban continental precipitation. In doing so, we are seeking to answer the following questions:

1. Does sulfate influence the ice nucleating processes in the study sites?
2. Does the source of the sulfate matter (i.e. sea-salt vs non sea-salt sources)? Will it correspond with known isotopic signatures of regional sulfate sources?
3. Does marine biogenic sulfate play an important role in Arctic ice nucleating particle characteristics? Are changes in these characteristics more evident for certain types of samples (i.e. fog, rain, or dry deposition)?

Chapters one and two set the scope of the research, presenting an in-depth review of atmospheric aerosols, their radiative properties, and their importance in mixed-phase clouds. A review of techniques for studying ice nucleation particles will be included, along with discussion of ice nuclei characteristics. Possible sources for sulfate, including biogenic sources like DMS will be covered, along with background information on sulfur isotopes and applicability of their specific isotope signatures. Chapter three reviews sampling methodology used in this particular study, and covers instrumentation for precipitation collection for Calgary, Kananaskis, and Arctic samples. The development of the droplet freezing technique instrumentation is covered, methodology review for anion/cation analysis, and isotope measurements. Chapter four includes results comparing filtered and unfiltered samples, comparisons of blanks (pure water) and samples, precipitation sampler comparisons, anion/cation concentrations, isotopic signatures and HYSPLIT back trajectory modeling. Chapter five covers discussion of the results, including comparisons between multi-year Arctic samples, urban vs rural continental samples, isotopic results, and

biogenic influences. Concluding remarks, as well as suggestions for further research are given in chapter six.

Chapter Two: Atmospheric Aerosols

2.1 Arctic Amplification and Aerosol Influences

With the rise of fossil fuel use, greenhouse emissions have continued to increase over the last century. The National Oceanic and Atmospheric Administration (NOAA) Global Monitoring Division has reported that CO_2 alone has increased from ~340 ppm to over 400 ppm from 1980-2018 (NOAA/ESRL Global Monitoring Division, Accessed December 2018). Based on a wide variety of plausible emission scenarios, many modeled approaches suggest that average surface temperatures could increase by as much as 6 ^{o}C by the turn of turn of the century (Riebeek, 2010; Woodard et al., 2019). To better understand these changes, scientists are increasingly more interested in studying geographic regions that exhibit highly variable climate feedbacks. With the Arctic region of the northern hemisphere exhibiting particularly sensitive feedbacks, changes are occurring at faster and more unprecedented rates in the past two decades (Maxwell, 1992; Koivurova, 2017). The ratio of Arctic change compared to global averages (Arctic amplification), has led to regional temperature increases which are double the global mean (IPCC, 2013). Additionally, modeled predictions suggest that the Arctic amplification ratio will continue to rise, more, than doubling the current rate of global surface temperature increases (Bony et al., 2006; Feldl et al., 2017).

As a predominantly snow-covered region, the Arctic's principal climate drivers are solar radiation and ice/snow cover. Fluctuations in these drivers regulate Arctic climate through surface heat/humidity exchange, balancing radiation budgets, and changes in surface albedo (Aagaard and Carmack, 1989). Decreases in albedo are of considerable importance in the Arctic region due to

large differences between summer and winter insolation (Koivurova, 2017). The ability for the surfaces at northern latitudes to reflect incoming radiation have lasting effects on amounts of heat which can be transferred to the surface and held within the Arctic hemisphere.

As variations in albedo continue to change, the presence of low-level clouds in the Arctic have been shown to have a significant contribution to Arctic surface warming (Intrieri et al., 2002, Gabric et al., 2018). Particularly, it is of significant interest to understand how surface cloud radiative forcing will affect polar regions. Using climatological cloud properties, past forcing has been modeled, showing that the average effects of polar clouds are to primarily to warm the surface over an annual cycle (Curry and Ebert, 1992). This cycle exhibits a net warming for much of the fall, winter, and spring. Conversely, the summer months have been shown to predominantly exhibit net cooling effects (Lewis and Curry, 2015).

With net fluctuations on surface temperatures primarily due to direct (scattering and absorption of sunlight) and indirect (alteration of cloud properties) aerosol effects, understanding the seasonal variations in aerosol sources becomes paramount in modeling accurate representations of the Arctic radiative budget. Since the 2013 IPCC report (IPCC, 2013), there have been numerous developments in estimations of direct and indirect aerosol effects, leading to more accurate models (Chen et al., 2018; Schultze and Rockel, 2018). These models can assist in more accurate estimations of aerosol contributions toward global annual mean radiative forcing as a result of present-day anthropogenic tropospheric aerosol concentrations.

Arctic anthropogenic aerosol models are a valuable tool to investigate how direct and indirect effects of aerosols influence radiation, clouds, and surface albedo. Anthropogenic aerosols have been shown to warm the Arctic atmosphere and have a cooling effect on the surface for all

seasons, with the largest forcing from black carbon (BC) (Quinn et al., 2008). Additionally, observations of surface sample sites have shown significant decreases in both sulfate and BC concentrations of up to 2-3% per year, consistent with GEOS-Chem transport model observations for 1980-2010 (Breider et al., 2017). These decreases in anthropogenic sulfate loading are suggested to be responsible for the net positive radiative forcing (warming). Similar trends in MSA have indicated that biogenic sources are likely to be responsible for climate change in the Arctic, and strongly influence sea ice melt and sea surface temperature increases (Breider et al., 2017).

Within the last half of the 20th century, countless studies have confirmed the ability of atmospheric aerosol particles to influence radiative forcing through the alteration of aerosol concentrations in low level clouds (Hansen et al., 1980; Haywood and Boucher., 2000; Kaufman et al., 2005; Huang et al., 2006). As a result of this significant ability of aerosols to influence the Arctic Haze and annual radiative budgets, it is critical to formulate a deeper understanding of atmospheric aerosols, analyze what sources they are produced from, and how they contribute to radiative forcing mechanisms.

2.2 Radiative Influences

Aerosols (colloidal suspensions of particles and/or liquids dispersed in air or gas) exist in the atmosphere in both natural and anthropogenic abundances. With a strong tropospheric presence, aerosols possess a strong ability to influence radiative forcing. These changes can manifest in direct radiative forcing from the absorption, and scattering of solar radiation, leading to effects such as sea level rise and melting ice cover. Aerosols can also indirectly influence climate through chemical and microphysical properties of aerosols, which influence radiative properties

of clouds, and how/when they form. The dominant control which aerosols display over clouds governs changes in how clouds can reflect, scatter, and transmit radiation. In turn, these changes can have lasting effects on climate on both regional and global scales.

Phase transitions exhibit a dominant role in climate properties through the formation of droplets and clouds, therefore making them critical influencers of climate (Hansen et al., 1980). In addition to their other properties, aerosols also have the potential to alter the chemical composition of the troposphere. These changes in lower atmospheric layers occur through the promotion of reactive heterogeneous chemistry and the scavenging of both semi volatile and acidic gas-phase trace species (Abbatt, 2003). Significant alterations to the troposphere can lead to drastic changes in properties influencing cloud formation, lifetime, precipitation capacity, and even albedo. The presence of ice crystals in mixed-phase clouds could also change properties in precipitating and nonprecipitating clouds. With the critical role that ice nucleation holds in the formation of precipitating low-level clouds, there is a high degree of importance associated with understanding how different aerosol sources can influence the ice nucleation process.

The role of aerosols in the growth and formation of low-level clouds is critical as a result of the strong climate influence of summertime cloud cover. Additionally, it is important to review the physical mechanisms that lead to the production of CCN (Cloud Condensation Nuclei) or IN (Ice Nuclei), and how their presence can induce changes on low level clouds in general. Delineation between CCN and IN will be presented, as well as the development of scientific literature concerning aerosol nucleation.

2.3 Cloud Condensation and Ice Nuclei

There are two main ways by which particles undergo nucleation. IN are particles that act as the nucleus for the formation of an ice crystal in the atmosphere and are typically closer to 0.5 μm in diameter. IN are generally insoluble aerosol particles which can include bacteria, leaf fragments, soot, and pollen. CCN are typically smaller (closer to 0.2 μm in diameter), semi- or fully soluble species upon which water vapor condenses. These can, for example, originate from pollution plumes (ex. organics, sulfates, or nitrates) or biogenic gases that undergo gas-to-particle conversions.

The ability for a CCN or IN to undergo activation (ice nucleation leading to precipitation) can be influenced via coatings of a soluble species. For example, sulfate coatings on dust or soot attract H_2O vapor, thereby enhancing growth and potentially activating the ice nuclei (Eastwood et al., 2009). Due to the solubility differences between CCN and IN, deeper understanding on their growth from aerosols is necessary to understand the evolution of clouds and precipitation.

2.4 Mixed-Phase Clouds

A mixed-phase cloud exists when there is a three-phase colloidal system, which is comprised of water vapor, ice particles, and coexisting supercooled liquid droplets. These systems are common throughout the troposphere and present at latitudes from polar to tropic regions. With such a large presence, mixed-phase clouds exhibit a critical role in precipitation, cloud persistence, and radiative budgets from a regional to global scale. (Korolev et al., 2017)

Due to the important role mixed-phase clouds play, it is important to understand the dynamics of aerosol-cloud interactions. Formation of these cloud types typically occurs in the lower troposphere at temperatures between 0 ^{o}C and -38 ^{o}C. With the remote nature of the Arctic, low level clouds over the frozen surface consist mainly of ice crystals and supercooled water, indicating an abundance of mixed-phase clouds.

Current descriptions of mixed-phase clouds are poorly represented in global climate models, leading to uncertainties in climate predictions (Fridlind and Ackerman., 2018). There also exists a generalization which indicates that global and regional climate models consistently underestimate the liquid condensate of the Arctic winter, leading to errors in estimations of downwelling radiation (Prenni et al., 2007; Karlsson and Svensson, 2011). These errors in atmospheric energy budgets result from poorly coupled models which do not properly account for accurate ice nucleation in mixed-phase clouds.

With the presence of water vapor, ice particles, and supercooled liquid droplets; absorption, reflection, and transmission within mixed-phase clouds is greatly affected by the dominance of a single phase. For example, liquid water clouds are optically thicker than ice clouds, which cause strong absorption of longwave radiation, leading to influences on sea ice coverage and thickness, even translating to effects on climate (Curry and Ebert 1990; Harrington and Olsson 2001). These variations prove exceedingly difficult to model due to the wide range of temperatures at which ice crystals form. Potential feedbacks have been mentioned where increased winter warming from greenhouse gases could cause a rise in the abundance of liquid water in mixed-phase clouds, thereby causing increases to the longwave radiation at the surface (Prenni et al., 2007). Furthermore, these model difficulties with Arctic clouds are suggested to result from inaccuracies in ice nucleation parameterizations. Detailed cloud-resolving model studies suggest that mixed-

phase Arctic clouds are extremely sensitive to minute changes in ice nuclei concentrations (Prenni et al., 2007).

2.5 Ice Nucleation

The ice nucleation mechanism occurs when favorable conditions are present (temperature, relative humidity, and existence of an appropriate nucleation surface). In the absence of an ice nucleating particle, pure water droplets can persist in a supercooled state to temperatures which approach -38 ^{o}C whereupon freezing occurs homogeneously (Kulkarni et al., 2014). The presence of ice nuclei in atmospheric water droplets serves to lower the energy barrier that must be surpassed in order to form ice crystals. This aids in ice nucleation at temperatures warmer than T= -38 ^{o}C. This process of forming ice crystals from an ice nucleating particle is referred to as heterogeneous nucleation. When ice nuclei are present, clouds dominated by ice particles have potential to exist at temperatures as warm as -10 ^{o}C. Several modes of heterogeneous nucleation can take place when aerosol particles are present and acting as ice nuclei. These modes are immersion, condensation, collisional/contact, and deposition-based freezing (Figure 2-1).

Immersion nucleation occurs when a solid particle within an existing droplet serves to act as a nucleus for the ice formation process, leading to the freezing of the droplet. Condensation nucleation occurs when water vapor condenses onto solid particles to form a droplet, leading to the particle to act as an immersion nucleus. Contact nucleation is when a solid particle is in collision with an existing droplet and the nucleation process is then initiated from that droplet. Deposition occurs when water vapor is deposited onto ice nuclei and proceeds directly to the crystalline form without existing in the liquid phase. It should be noted that although deposition

mode nucleation is theoretically possible, current experimental evidence supporting the importance of this process in the atmosphere is lacking (Marcolli, 2014).

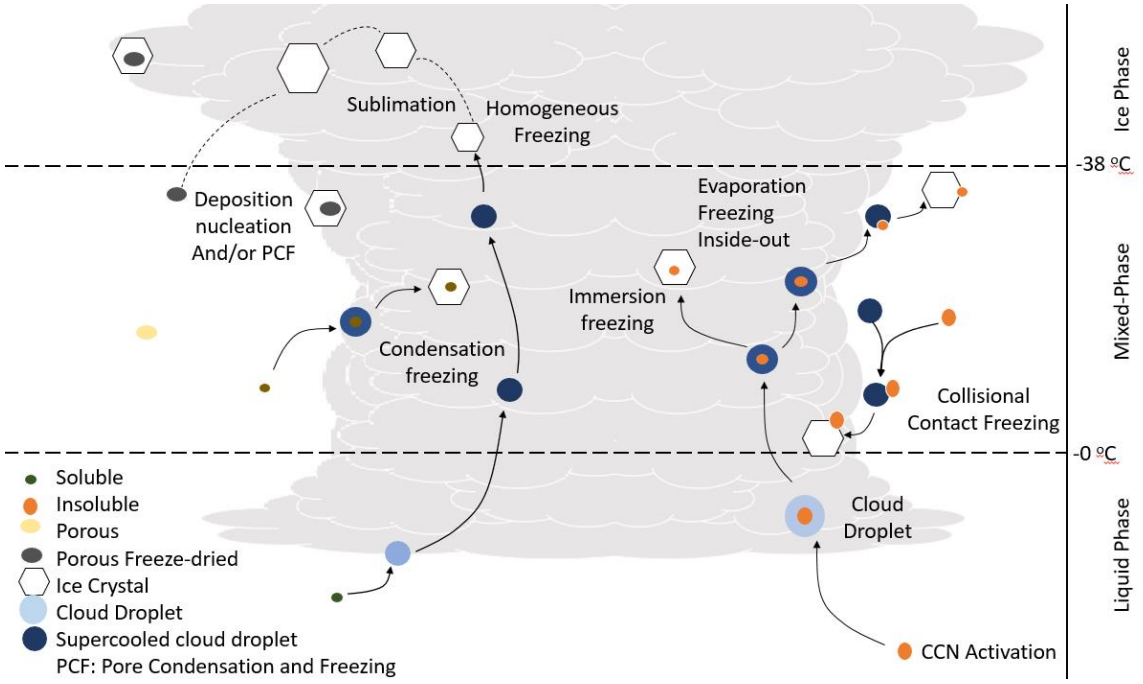

Figure 2-1. Primary ice nucleation modes in the Atmosphere (after Kanji et al., 2017).

The specific properties which are required for aerosol particles to act as ice nuclei are not yet fully understood, with significant differences in formation conditions being required for each of the specific modes listed above. Additionally, the atmospheric conditions which lead to the different modes of nucleation could vary for the same particle, leading to the need for supplementary laboratory studies on the nucleation of different aerosol particles. As measurements of ice nucleating particle concentrations in clouds vary by several orders of magnitude 10^1 to 10^8 INP/L from -5 to -38 ^oC, it becomes difficult to perform accurate studies outside of the lab (Welti et al., 2018). Vapor diffusion causes crystals to grow rapidly following the initial nucleation process, and the ability of secondary ice production from existing ice crystals

causes direct measurements to become very difficult. Fracturing of evaporating crystals, inter-particle collisions, and vapor deposition all take place quickly following primary nucleation mechanisms. Due to the fast-paced growth that takes place, laboratory studies concerning these particles remain important to further explain these basic mechanisms that cause the initial nucleation from aerosols.

2.6 Ice Nucleation Measurement Techniques

There is general agreement that aerosols nucleate in two major ways, and as such, studies are divided by two overarching groups. Wet dispersion first involves dispersion of ice nuclei into water. The droplets formed are then frozen and subsequently studied. The second method is dry dispersion, which involves the dispersion of aerosol particles into the air where they are activated into water droplets before the freezing process. The raw nucleation data obtained from either method are given as a fraction of droplets frozen under certain conditions. This leads to information about the activity of the nucleating particles, and the importance of modifications to the numerous physical variables imposed upon the particle at the time of nucleation. The most common variables used in nucleation experiments are temperature, cooling rate, droplet size, particle size, aerosol source, and relative humidity.

2.6.1 Wet Dispersion Methods

Wet dispersion experiments are typically some version of a droplet freezing experiment. Typically, samples are divided into subsamples representing size segregation, source region, and other climatic factors. Samples are then cooled down at variable freezing rates until ice crystals appear, yielding the activation percentage of droplets which freeze at certain conditions. As a result, temporal data linked to each of the changing attributes is critical. Freezing typically occurs via a hydrophobic stage with wells or vials, with small sub-microliter droplets. Aerosol particle sizes typically do not exceed the picoliter to nanoliter range.

For consistency, the freezing rates in IN experiments are typically linear, although rates following temperature isotherms have also been used to investigate more aggressive rates of cooling. Recently, more complex studies have taken place, introducing the use of wind tunnels, repetitive freezing of samples, and electrodynamic levitation. With the introduction of new parameters, atmospheric conditions can be more accurately simulated (Stöckel et al., 2005).

2.6.2 Dry Dispersion Methods

Dry dispersion involves the use of flow chambers which allow for scientists to control the temperature, humidity, and aerosol contents with the goal of simulating actual cloud conditions. Through evacuation, ice nucleation conditions can be introduced to the sample chambers, indicating the presence of ice nuclei from visible crystallization. As the aerosols are typically not immersed in droplets yet, these experiments involve an extra step. The inclusion of a cold stage transforms the aerosol particles into cloud condensation nuclei first through changes in the relative

humidity. With this initial step occurring before ice nucleation processes begin, this method allows for a more isolated approach to exploring the complex nucleation pathways shown in Figure 2-1. A particularly effective instrument that has become quite popular in dry dispersion experiments is the utilization of Continuous Flow Thermal Gradient Diffusion Chambers (CFDCs), which allow for the segregation of aerosol size, concentration, and saturations. In addition to providing better control over the nucleation process by using flow-through methods, this instrumentation allows for more accurate simulation of real-time atmospheric conditions. Utilization of CFDCs can provide observations of pre-activation of aerosols to cloud condensation nuclei for a more comprehensive exploration of the immersion-based pathways illustrated in Figure 2-1. A complex overview of CFDCs for ice nucleation purposes by Rogers (1998) is a valuable resource for those undertaking this method. It is valuable to note that although comprehensive, development of these systems is considerably more complex and costly than widely accepted dry deposition techniques.

2.7 Effective Ice Nuclei Properties

The capacity of a particle to react to the moisture content of the air via absorption or release of water vapor is referred to as the hygroscopicity. With factors like size, shape, surface texture, and conductivity all influencing the ability of aerosols to nucleate, it is desirable to definitively categorize which attributes exhibit a dominant capacity during nucleation events. Unfortunately, it is currently not possible to describe the activity of ice nuclei with a single hygroscopicity parameter (Petters and Kreidenweis, 2007). While this sort of description is available for CCN, the ability to apply this to ice nuclei has proven more difficult in the past decade (Tang et al., 2016). While deposition mode ice nucleation be linked to pore-condensation freezing, immersion

freezing mode is the most important freezing mode within mixed-phase clouds (Augustin-Bauditz et al., 2014; Campbell et al., 2016; Marcolli, 2014). The dominance of immersion freezing is determined by the soluble fraction of aerosol particles. For low soluble fractions, contact freezing dominates the freezing process, and holds lower dependence on both temperature and aerosol particle type. Higher soluble fractions lead to immersion freezing with a strong temperature dependence (Diehl et al., 2006).

The small spatial extents of the ice nucleation events, as well as the small size of the critical ice nucleus both contribute to the difficulty in measurements of ice nucleation parameters. This size dependence as a function of temperature for pure water is shown explicitly in Figure 2-2, where the dependence ranges from a 1 nm radius nucleus at -38 ^{o}C to a 10 nm radius at -4 ^{o}C. As a result of the specific criticality, these optimal radii are rare when compared to the relative abundance of ice nuclei. This low abundance of critical radii usually results in the presence of only a single critical radius in each droplet which freezes. As a result, there is currently no technique capable to locating the active nuclei for the droplet. The resulting effect of this is that most current physical information about the properties of ice nuclei have been inferred from experimental data. To offer more insight to this, the five properties Pruppacher and Klett (1997) thought to be important for heterogeneous nucleation are as follows:

1) Insolubility requirement: Nucleating surfaces need to provide an interface with water. Dissolved substances (CCN) do not provide an effective ice nucleation interface.
2) Size Requirement: Atmospheric observations indicate that IN tend to be large. Although vague, this requirement is rooted in observations that larger particles in the atmosphere tend to be the nucleating ones. Another assumption is that an ice nucleating particle must be larger than a critical nucleus.

3) Chemical bond requirement: The ice nucleating particle is required to be able to bond with water for nucleation to take place. The stronger bonds are assumed to improve the nucleation efficiency.
4) Crystallographic requirement: Substances with a similar lattice structure and similar spacing to ice will provide a more ideal template for a critical nucleus
5) Active site requirement: Site specific descriptions have been observed to often give the best account of ice nucleation. Furthermore, deposition mode ice nucleation frequently occurs at specific locations on ice crystals. It is hypothesised that this condition is more related to vapour condensation than ice nucleation (Marcolli, 2014)

Ice nuclei are typically larger and insoluble when compared to cloud condensation nuclei (Pruppacher and Klett, 1997). Certain biological materials have recently been proven to be effective as ice nucleating particles (Pummer et al., 2012, 2015). On average these particles display a mean size of less than 10 nm, which is only slightly larger than that of critical ice nuclei. This size dependence can be seen explicitly in Figure 2-2. The chemical bond requirement is important since the ability for water to bond to nucleating particles is critical. It is well understood that a hydrophilic surface should be able to nucleate ice more efficiently than that of a hydrophobic surface. While there are few experimental studies of the relative surface-characteristic variations of hydrophilicity, these characteristics remain exceedingly challenging and difficult to test. Comparisons of the nucleating ability of hydrophobic and hydrophilic surfaces have been conducted, with hydrophobic surfaces typically exhibiting more suitable ice nucleating surfaces (Alizadeh et al., 2012). In addition, specific studies on the nucleation of hydrophobic vs

hydrophilic soot's have proven to favor the latter as a more efficient site of nucleation (Gorbunov et al., 2001).

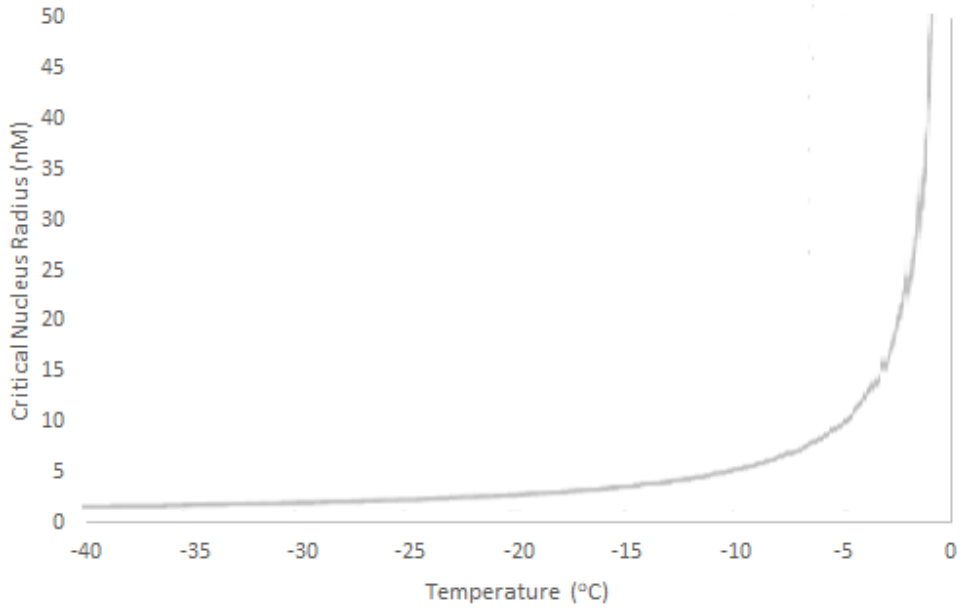

Figure 2-2 Critical radius size for ice nuclei as a function of temperature. (After Pruppacher and Klett, 1997).

The lattice structure and topographical features of an ice nucleating surface are also widely considered to be principal factors (Pruppacher and Klett, 1997). Similarities within the crystal structure of the nuclei to ice should assist in the bonding for the initial layer of ice. This lattice matching is possible to be calculated from existing knowledge of the crystalline structure. These predictions have been previously performed and matched in subsequent experimental studies of Silver Iodide (AgI) (Vonnegut, 1947). It is important to note that while similar attempts to match lattice predictions have been made on BaF_2, subsequent experimentation has failed to confirm this (Marcolli et al., 2016). These experiments show that although there is some evidence to support

certain parameters of good ice nuclei, much uncertainty remains in current research. In addition to this, there have also been subsequent studies suggesting alternative mechanisms for the nucleation of ice. In the case of AgI, it has been suggested that factors like surface charge could in fact control the nucleation process (Marcolli et al., 2016). The final requirement suggested by Pruppacher and Klett comes from the argument that the surfaces of the nucleating particles must contain active sites, and that depositional mode nucleation occurs on very specific sites which depend on the species of nucleating surface (Herbert et al., 2014; Vali, 2008, 2015). Additionally, it has been suggested that there are differences in location of depositional versus immersion nucleation sites, with the former mode forming ice crystals more slowly (Gurganus et al., 2011; Gurganus et al., 2013; Gurganus et al., 2015). As Gurganus and his colleagues have demonstrated this is possible to observe through immersion mode systems with the use of high-speed cameras.

Despite advances in technology (CFDCs), there is still a general uncertainty regarding the factors that lead to effective ice nucleation. As a result of these uncertainties, many studies in recent years have placed a stronger focus on developing understandings of aerosol species responsible for ice nucleation within mixed-phase clouds.

2.8 Aerosol Sources

As previously mentioned, there are a host of laboratory studies that have observed the immersion mode nucleation to quantify and explain how various sources of aerosols could nucleate ice in the atmosphere.

The emission of mineral dusts from desert regions in Africa and Asian are known to be large sources of ice nuclei (DeMott et al., 2003). For numerous years, it has been well understood

that snow crystals contain the residues from mineral dusts (Kumai, 1961). Furthermore, it has been shown that mineral dusts are a large constituent of ice crystals in certain cloud types (Murray et al., 2012). Within the family of mineral dusts, it was previously suspected that clay minerals were responsible for the activity of ice nucleation from mineral dusts (Lüönd et. al 2010; Pruppacher and Klett, 1997). More recently this attitude has come around with others (Atkinson et al., 2013) confirming how feldspar aerosols are much more efficient at nucleating ice. These recent studies go on to suggest that indeed feldspar aerosols (Na/Ca, Montmorillonite, Kaolinite, Quartz, Mica, Calcite, Chlorite) are likely responsible for much of the ice nucleation at regional and global scales (Atkinson et al., 2013).

In addition to mineral dusts, much work has been done on the ice nucleation activities of biological entities. One of the first instances of this work was the work of Schnell and Vali (1975), where the decomposition of leaf matter was observed. This study showed ice nucleation from the decomposition of leaf matter induced freezing at higher temperatures than other tested particles. Because of this work, more focus was placed on studying the organic matter which could include ice nucleation events (in the case of the Schnell and Vali's work, the plant pathogen *Pseudomonas Syringae*). Since this discovery, many other bacteria have been shown to nucleate ice at higher temperatures than homogeneous freezing mechanisms (Hansen et al., 1990).

Other effective nucleators include fungi (O'Sullivan et al., 2014), pollen (Pummer et al., 2012;2015), and plankton (Alpert et al., 2011; Knopf et al., 2011; Schnell, 1975). Additional contributors to the global aerosol budget are anthropogenic burning of fossil fuels and the destruction of biomass (Bond et al., 2013). Studies comparing the relative effective nucleation of different particles (i.e. soot particles vs biomass aerosols) have also been conducted (DeMott, 1990; Diehl and Mirta, 1998; Gorbunov et al., 2001). Despite comparative studies, quantification

of IN effectiveness remains complicated, with comparisons between different instruments yielding results of variable reproducibility (Hiranuma et al., 2015). Aside from complicating comparisons, this suggests accurate parameters governing ice crystal formation is lacking. Despite this, it is possible to speak toward the general effectiveness of an aerosol species nucleation activity (Murray et al. 2012). More difficulties arise due to temperature variations and droplet sizes between different studies. While biological nucleators tend to be tested with larger droplet sizes, their non-biologic counterparts tend to be tested with smaller sized droplets (Kanji et al., 2015). In consideration of Figure 2-3, it is clear how comparisons of nucleating species can be valuable, especially with definite trends emerging in comparisons of biological nuclei with their mineral counterparts.

From Figure 2-3, *P. Syringae* exhibits nucleating ability far above the others, with nucleation occurring at far warmer temperatures. The BCS 376 microcline in Figure 2-3 is the alkali feldspar (Atkinson et al., 2013), which is by far the most effective of the mineral groups presented, dominating the non-biological aerosol. Atkinson (2013) suggested that the feldspar attribute was the dominating particulate component leading to nucleation in several other mineral samples (dessert dusts and kaolinite samples to name a few). Despite this, Figure 2-3 indicates that even the weakest nucleating biological species exhibit a stronger nucleating ability than that of the mineral species, leading the authors to the conclusion that bacterial aerosols are more effective at ice nucleation. While this is a clear statement toward the obvious effectiveness of biological species to nucleate, there is still some debate surrounding the relative importance of specific aerosol species. This uncertainty is due to highly variable particulate concentrations in the atmosphere. For instance, some studies suggest that mineral dusts are globally dominant for the formation of mixed-phase clouds. However, there remains some disagreement in the literature,

where others have suggested that biological species could in fact play a larger more critical role on a global scale (Hoose et al., 2012). Ultimately these uncertainties arise from a lack of laboratory and field measurements which could serve to offer a more concrete comparison. With contrasting opinions about the relative importance of feldspar mineral aerosols and marine biological components, the overall precise identity of primary ice nucleating particle drivers is still unknown. While this seems to indicate a lack of knowledge toward the drivers of ice nucleating particles, much progress has been made in explaining underlying physical mechanisms through the study of specific aerosol species.

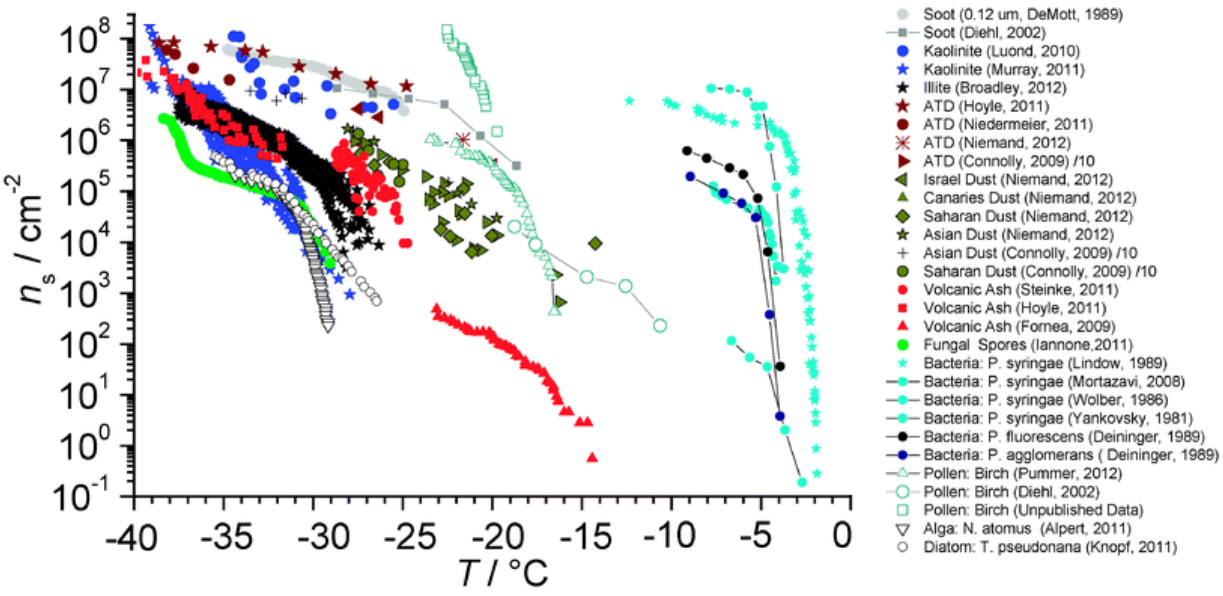

Figure 2-3 Ice nucleation efficiencies for a wide range of nucleators based on studies spanning the past ~50 years. Bacterial nucleators clearly exhibit a dominance when considering the sheer effectiveness, the ice nucleating particle species (after Kulmala et al., 2013).

2.9 Arctic Biogenic Sulfate

Dimethyl Sulfide (DMS) produced from marine phytoplankton metabolic compounds is one of the most abundant forms of sulfur released from the Arctic ocean (Becagli et al., 2016). The drastic decline in sea ice thickness, coverage, and extent is expected to lead to a substantial increase in production biologically produced sulfate. Oceanic sources transport aerosols like sea spray and DMS into the atmosphere rapidly at the surface of the ocean through the bubble bursting illustrated by Pruppacher and Klett (1997) in Figure 2-4. Once the bubble propels the DMS into the atmosphere, it is oxidized, giving way to sulfate and MSA (methane sulfonate aerosols). These aerosols can then go on to form cloud condensation nuclei as discussed earlier. The production of this biologic aerosol has been the topic of some debate in recent years, with feedback loops initiated by the cloud condensation nuclei called into question (Becagli et al., 2016).

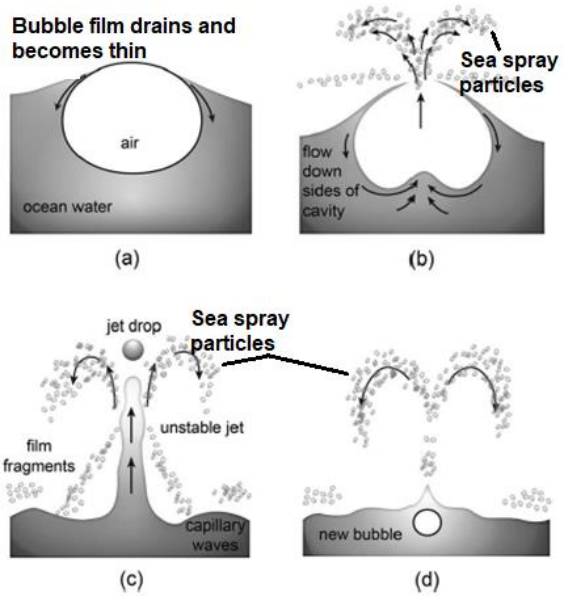

Figure 2-4 Bubble bursting mechanism of marine based aerosol particles. (After Pruppacher and Klett, 1997).

2.10 Arctic DMS and the CLAW Hypothesis

While research on ice nuclei is still under constant review (Vali et al., 2015), many studies in the Arctic have had a strong focus on the sea surface microlayer and bulk seawater influences on ice nucleating particles production. Of particular interest is how these biological sources influence the mixed-phase clouds in the Arctic. As mentioned earlier, the ability of ice nuclei to freeze and form ice crystals at temperatures warmer than -38 ^{o}C allow for influences over Earth's climate and the hydrological cycle through the alteration of microphysics, radiative properties, and cloud lifetime (DeMott et al., 2010). Modelling studies further support the need for research into ice nucleating particles and marine sources, with modeled results suggesting that the ocean can be a dominant source of ice nucleating particles in the atmosphere in regions where dust concentrations are low, like the Arctic (Levasseur, 2013). While this field of research is relatively recent, there has been some debate within the scientific community surrounding the influence which biological particles can have on cloud condensation nuclei rather than ice nuclei.

Throughout the past two decades, there has been a significant amount of interest in studying DMS contributions toward radiative forcing. Observations in the marine boundary layer, laboratory studies, and modeling efforts have all been conducted to find evidence for the linkage between biogenic aerosols and radiative forcing. The first proposal of this linkage was the CLAW hypothesis, proposed by Robert Jay Charlson, James Lovelock, Meinrat Andreae, Stephen G. Warren (named from the first letter of the surnames). (Charlson et al., 1987). The hypothesis (Figure 2-5) described a feedback loop that starts from increasing sea surface temperatures and solar insolation increases the growth of phytoplankton. This increased phytoplankton activity leads to the production of dimethylsulfoniopropionate (DMSP), and thereby the breakdown product DMS. The DMS is oxidized in the atmosphere in order to form sulfur dioxide, and thereby sulfate

aerosols. These aerosols, once present in the atmosphere, can act as CCN or IN. In turn, this has an effect on liquid water content, and ice crystal content in clouds, leading to increases in radiative properties of clouds (albedo and reflection of incident sunlight).

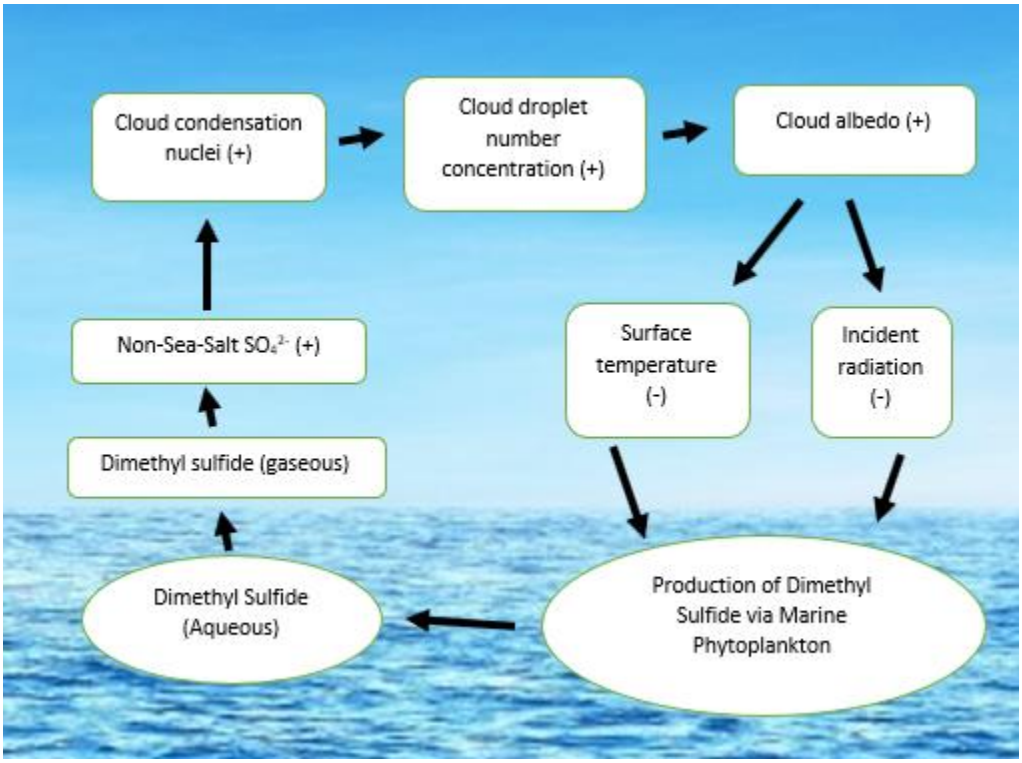

Figure 2-5 Climate feedback loop proposed in the CLAW hypothesis (After Charlson et al. 1987).

While the CLAW hypothesis delivered a valuable framework for global climate models to incorporate feedbacks, this has been difficult to implement because of the range in scale (from nm to global scales), much work has been done in recognizing the differences of feedbacks resulting from DMS production at regional scales instead. There is still a large debate in the role of anthropogenic and biogenic sourced sulfate in the Arctic feedback loop (Figure 2-5).

Understanding the specific roles of non-sea salt sulfate is therefore key in providing better clarity in understandings of the Arctic feedback. Currently, the non-sea salt sulfate is primarily dominated by anthropogenic sources. Additionally, there is still uncertainty in associations between DMS flux, changes in the sea ice extent, and phytoplankton productivity (Abbatt et al., 2018). With large declines of thick (>2m) multiyear ice, biological production along the sea shelf is increasing (Gabric et al., 2018). With regional warming and decreases in sea ice extent, it is expected that increases to net phytoplankton production of 20-30% could occur (Arrigo and van Dijken., 2015). Furthermore, as a result of the magnified source strength of the primary organic biological particles and DMS, an increase in oceanic influence on atmospheric composition is to be expected (Orellana et al., 2011; Almeida et al., 2013). Specifically, it has been suggested that seasonal DMS emissions vary in influence, with many models proposing weaker climate feedbacks in summertime due to more effective aerosol removal (wet removal, limited transport from lower latitudes, and diminishing new particle formation) (Croft et al., 2016)

While increased cloud cover can cause greater absorption of solar energy, this causes adverse effects in the Arctic climate. Due to the predominantly ice- and snow-covered surface, increased cloud cover can serve to warm the surface by more effectively trapping portions of the outgoing long wave radiation. In fact, it has been shown that cloud cover in the Arctic has increased in recent decades (Döscher et al., 2014)

Indeed, studies suggest that DMS emissions play a larger role in climate change in remote areas with low aerosol concentrations and have shown to have negligible impact on regional scale climates (Levasseur, 2013). Furthermore, anthropogenic and biogenic sulfate can act as a proxy for acidic and organic compounds. The sea spray aerosol mentioned earlier includes the sea salt and organic compounds that act as the main source of aerosol marine environments such as the

Arctic (DeMott et al., 2016). With the ability for viscous organic aerosols to facilitate heterogeneous ice nucleation (Ignatius et al., 2016), sources of sulfate like DMS can act as a proxy for processes and conditions which occur on the surface of aerosols, leading to potential influences on nucleation. These contributions of biogenic and anthropogenic sources on the formation and growth of sulfate aerosols in the Arctic have been shown before (Ghahremaninezhad et al., 2016), with dominant sources of fine particles (<0.7 micrometers) to be biogenic (>63%).

Additionally, high summertime DMS levels have been identified in ocean water and overlying atmosphere in the Canadian Arctic Archipelago, likely influenced strongly by the increasing prevalence of melt ponds (a major source of DMS). This particularly important in regions where more dominant mineral dust concentrations are low, presenting opportunity for the DMS to be more dominant (Abbatt et al., 2018).

The only way to further understand this is through deeper understandings of biogeochemistry and climate physics. This interdisciplinary research to uncover these relationships is now more important than ever with modern climate change.

2.11 Sulfur Isotopes

The use of sulfur isotopes offers a powerful method of differentiating aerosol sources through comparison of its stable isotopes. With constant number of protons, variations in number of neutrons in the nucleus corresponds to different isotopes. These differences are primarily the result of isotope fractionation due to chemical, physical, and biological reactions. Within nature, four stable isotopes of Sulfur can be found: ^{32}S (95% abundance), ^{33}S (0.75% abundance), ^{34}S 4.20% (abundance), and ^{36}S 0.017% (abundance). As a result, the isotope abundance ratios of the

two primary isotopes ($^{34}S/^{32}S$) are most commonly presented in comparison to an international standard, Vienna-Canyon Diablo Troilite (Krouse et al., 1991).

$$\delta^{34}\,S\,(‰) = \{\frac{\left(\frac{(^{34}S)}{(^{32}S)}\right)\text{sample}}{\frac{(^{34}S)}{(^{32}S)}\text{ standard}}) - 1\} \times 1000 \quad (1)$$

Within the Arctic, there are three major atmospheric sources of sulfate that must be considered (Figure 2-6). The major sources are anthropogenic sulfate with δ^{34} S = +3 ± 3 ‰ (Li and Barrie, 1993; Nriagu and Coker, 1978; Norman et al., 1999), biogenic sulfate with δ^{34} S = +18.6 ± 0.9 ‰ (Sanusi et al., 2006; Patris et al., 2002), and sea salt sulfate with δ^{34} S = +21.0 ± 0.1 ‰ (Rees et al., 1978). Conversely, Western Canada (Alberta) has been measured to have sour gas flaring and processing emissions (for well mixed air) with δ^{34} S = +18 to +30 ‰ (Norman et al., 2004), and vehicle exhaust at δ^{34} S = +5 ± 0.5‰ (Norman et al., 2004). Using these well studied sources, source apportionment methods can be used to identify sulfate fractions of aerosols in samples.

$$[SO_4^{2-}]_{\text{total}} = [SO_4^{2-}]_{\text{bio}} + [SO_4^{2-}]_{\text{anthro}} + [SO_4^{2-}]_{\text{ss}} \quad (2)$$

$$[SO_4^{2-}]_{\text{total}}\delta^{34}S_{\text{total}} = [SO42-]_{\text{bio}}\delta^{34}S_{\text{bio}} + [SO_4^{2-}]_{\text{anthro}}\delta^{34}S_{\text{anthro}} + [SO_4^{2-}]_{\text{SS}}\delta^{34}S_{\text{ss}} \quad (3)$$

Sea salt (SS) and non-sea salt (NSS) sulfate in samples was also calculated using the SO_4^{2-} and Na^+ mass ratios.

$$[SO_4^{2-}]_{ss} = 0.252[Na^+] \quad (4)$$

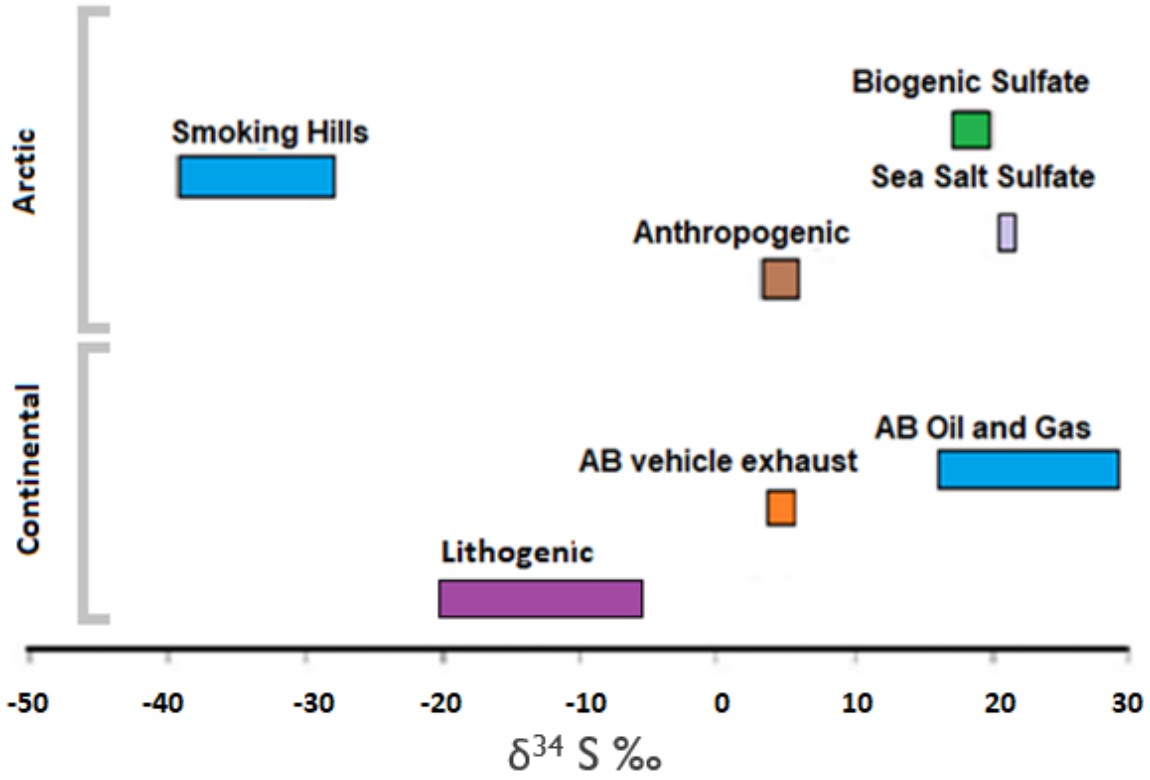

Figure 2-6 δ^{34} S values for sulfur sources in the Arctic atmosphere, along with urban sulfate sources for Alberta. Sea salt (Rees et al., 1978), DMS (Calhoun, 1990), Biogenic sulfate (Patris et al., 2000), Smoking Hills (Rempillo et al., 2011), Anthropogenic (Norman et al., 1999), AB vehicle exhaust and AB Oil and Gas (Norman, 2004).

2.12 Study Objectives

From the articles above, it is clear the immersion mode ice nucleation plays a critical role in how mixed-phase clouds evolve. With the uncertainty which is attributed to many of the physical properties which contribute to ice nucleation, it becomes more valuable than ever to explain the complex physical interactions which lead to nucleation from dissimilar sources. Additionally, it is exceedingly valuable to attribute relative importance to each source of aerosol within the marine boundary layer. Despite this, an overwhelming lack of data is present, making meaningful comparisons difficult. For the purpose of this study, three main objectives were identified:

1. Identify the influence of sulfate in the ice nucleation process in the Arctic and both rural (Kananaskis) and urban (Calgary) continental study sites.
2. Investigate connections between sulfate sources and study sites
3. Explore linkages between biogenic sulfate and changes in ice nucleation characteristics.

Exploring these objectives offers the chance for clarification of the relative importance of each individual aerosol species, assigning effectiveness of the particles to serve as Ice Nucleating particles. Through studies of this type, a greater understanding of why certain particles nucleate into ice crystals (under certain conditions) can hopefully be obtained. Coupled with development of more rigorous mathematical simulations, measurements of ice nucleating particles will assist in modeling and predicting growth, lifetime, and movement of mixed-phase clouds. These predictions will undoubtedly prove invaluable as effects from climate change become more severe, no doubt assisting in developing preemptive policies and frameworks to combat rapidly evolving climates.

Chapter Three: Study Site, Sampling and Analysis Methodology

3.1 Arctic Precipitation Samples

Precipitation samples from the Arctic (rain, dry deposition, and fog) were collected aboard the *CGS Amundsen* as part of a shipboard campaign (Figure 3-1) from June 10th to June 23rd (2014) and June 16th to August 23rd (2016), as part of the larger NETCARE objective (Network on Climate and Aerosol: Addressing Key Uncertainties in Remote Canadian Environments).

a)

b)

Figure 3-1 CCGS Amundsen research campaigns from 2014 (a) and 2016 (b).

Wind speed, direction, and sea surface/air temperatures were measured using the onboard Automatic Voluntary Observing Ships System (AVOS) held ~23 m above sea level. Measurements were collected every minute, and then averaged over a 10-minute window.

For both the 2014 voyage, the samples were collected using a passive rain sampler constructed from the top half of a 18.9 L water jug and held in place by a brace (Fig 3-2). During the 2016 voyage, the samples were collected using the passive rain sampler (Fig 3-2), in additions to a passive fog collector (Fig 3-3) on which fog droplets are deposited on vertical Teflon fibers (Schemenaur, 1986) that was set up above the bridge and mounted on a stand attached to a railing approximately 1 m above the surface of the roof of the bridge. When fog was present samples were collected using the fog sampler and the sampling conditions were noted in the precipitation sampling log along with the sampler type. When rain and fog were present, samples were collected by both sampling units for comparison and described as "rain and fog" and the collection device was recorded with the sample type and date. When rain was present, both samplers were again used to collect the sample "rain" and either "fog and rain collector" or "rain collector" and the date were recorded. Precipitation and fog were collected simultaneously when both events occurred during a set sampling interval. Blanks (consisting of deionized distilled water passed through the sampler following rinsing procedure) were taken along with samples on August 23rd, 2016.

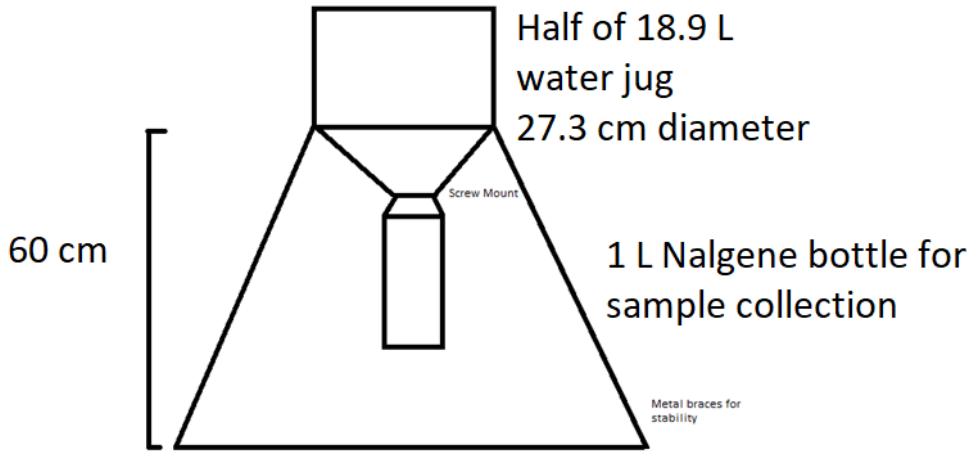

Figure 3-2 Passive precipitation sampler (VW) used for both Arctic and Urban (Calgary) and Rural (Kananaskis) continental samples.

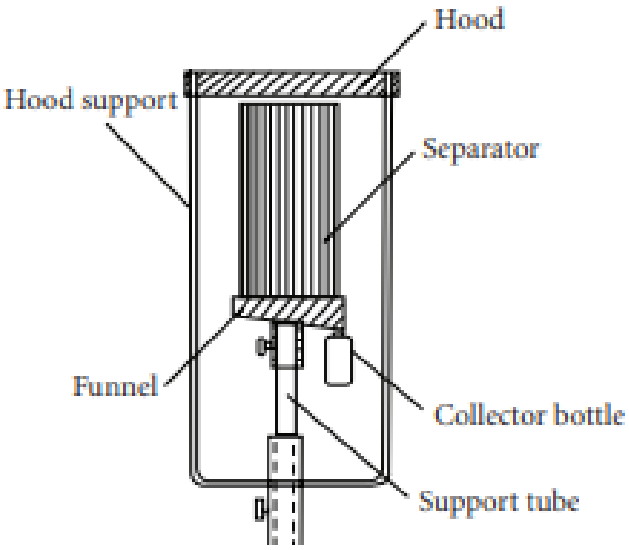

Figure 3-3 Shipboard fog/rain collector (EC) used during the Arctic 2016 shipboard campaign.

3.2 Kananaskis/Calgary Precipitation Samples

Dry deposition and wet deposition samples (rain and snow) were collected from 2016 to 2017 at the university of Calgary campus (urban site), as well as the Barrier Lake Station (Rural mountainous site) in Alberta, Canada.

The Calgary sampler was located roughly 20 m off the ground on the rooftop of the Science B building at the University of Calgary campus. The passive rain collector was the same as the Arctic sampler mentioned above (Figure 3-2). Following collection, the sampler was rinsed with Deionized-distilled water in order to prepare the collector for a fresh clean sampling environment. Collected samples were packed in sealed vials and stored in a refrigerator set to 4 ^{o}C.

Volume of samples were noted in order to indicate size of precipitation events, and then separated into vials for IN experimentation, IC analysis, and Isotope analysis. For IN experiments, some samples were tested for IN properties in filtered vs unfiltered samples. The criteria for sample selection was large precipitation events that provided samples which exceeded 300ml in sample volume.

3.3 Ice Nucleation Experiments

Following the droplet freezing technique (DFT: Koop et al., 1998; Vali, 1971; Whale et al., 2015; Wilson et al., 2015), samples were first homogenized by inversion, and between 10-20 ~ 1μL droplets of sample were deposited onto a glass slide using a 10 μL syringe with 0.2 μL increments. The slides were then placed into a sealed chamber attached to a cold stage (Figure 3-4), where a combination of a Peltier thermo electric cooler and coolant circulation unit were used

to cool the droplets at a rate of ~10 ^{o}C / min from 0 to -39 ^{o}C (Koop et al., 1998), under observation of a digital camera connected to a microscope. Cooling rates smaller than 2 ^{o}C /min and exceeding 10 ^{o}C/min have been shown to be unrepresentative of ice nucleation results. The errors present in rates 2 ^{o}C $< T$ ^{o}C < 10 ^{o}C /min are primarily due to the stochastic nature of the ice nucleation process along with measurement delays (exacerbated at larger cooling rates) between the cooling stage surface and location of the thermocouples (Koop et al., 1998). Each experiment was repeated 3 times and averaged for representative results. Following video analysis, the concentration of INP's as a function of temperature was determined from the following equation (Vali, 1971).

$$INP(T) = -\ln\left(\frac{N_u(T)}{N_o}\right) N_o * \frac{1}{V}$$

Where $N_u(T)$ is the total number of unfrozen droplets at a certain temperature T. N_o is the total number of droplets used in each trial, and V is the total volume of the droplets used in the trial. This equation accounts for the possibility of multiple INPs contained within a single droplet.

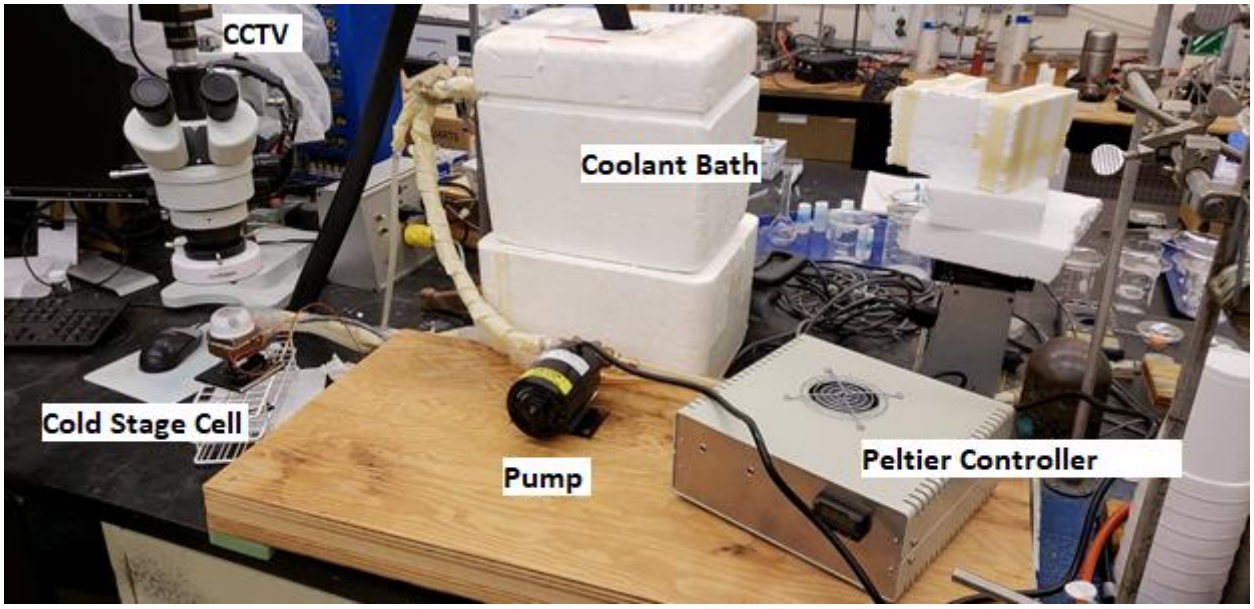

Figure 3-4 Apparatus developed for measuring INP(T) values for samples.

Measurements of ice nucleating particle concentrations as a function of temperature (INP(T)) were obtained through development of instrumentation in the lab (Figure 3-5). A microscope with a digital camera was combined with a cold stage which was connected to a thermo electric Peltier unit in conjunction with a circulating bath cooled with a Cryocool 100 unit to achieve sufficiently cold temperatures at appropriate rates. Unlike many typical freezing experiments (Kanji, Z. A., and Abbatt, J. P. 2006), a single cooling unit was unavailable for the range required in typical IN experiments (0 ^{o}C to < -38 ^{o}C). As a result, it was necessary to use a combination of a Peltier thermo electric cooler and a circulation bath combined with an immersion cooling probe to reach sufficiently cold temperatures (<-38 ^{o}C). The Cryocool 100 unit used has a set rate of cooling (Fig 3-6), which exceeded that of typical experimental rates of <10 ^{o}C / min. Therefore, it became necessary to add a new primary cooling unit that could be aided by the Cryocool unit. A thermo-electric Peltier cell was used to finely modulate temperatures of a cold

stage, while modulated inclusion of the Cryocool unit allowed for rougher temperature modulations. This combination allowed the cold stage to be cooled to -40 ºC at a constant rate of ~10 ºC / min.

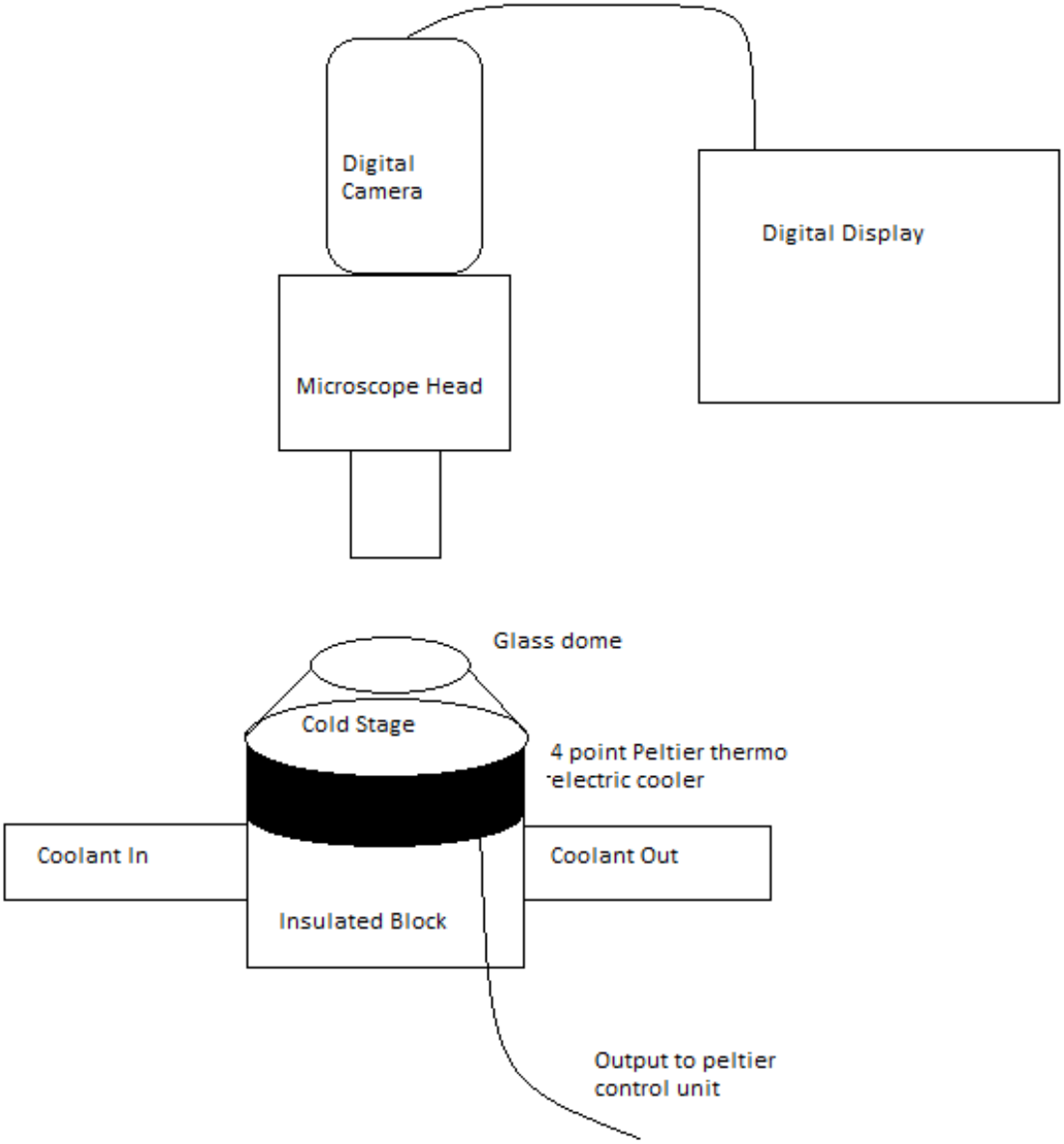

Figure 3-5 Schematic of Cooling stage apparatus. Samples were deposited on a glass slide which was then placed underneath the glass dome on the cold stage and monitored to calculate INP(T) concentrations.

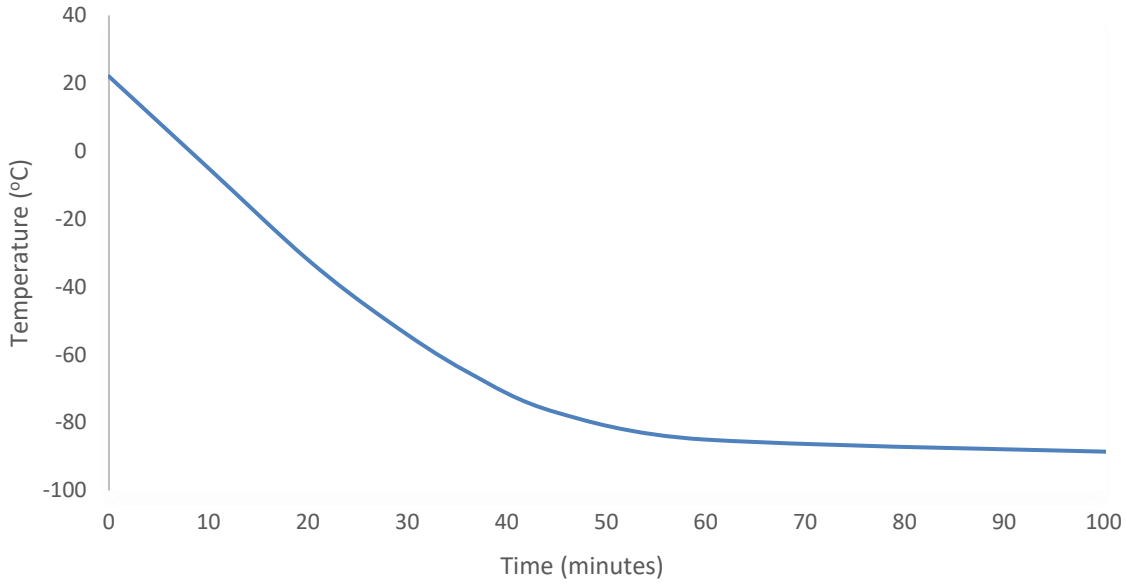

Figure 3-6 Cryocool 100 cooling curve. A Cryocool 100 unit was used in combination with a Peltier thermo electric cooler to achieve cooling rates between 5 < 10 ºC/min.

3.4 Cation/Anion Analysis

Ion chromatography was used to determine concentrations of cations (Ca^{2+}, K^{+}, Na^{+}, Mg^{2+}) and anions (Cl^{-}, SO_4^{2-}, Br^{-}, NO^{3-}) with a detection limit of 0.1 mg/L. Samples were first filtered through glass filters (Whatman glass microfiber filters, 47 mm diameter, 0.40 µm pore size) and submitted (10 ml volume of sample) for ion chromatography analysis.

3.5 Sulfate Analysis

In the laboratory, samples were combined with 5 ml of 10 % $BaCl_2$ and 1 ml HCl in order to precipitate $BaSO_4$ for $\delta^{34}S$ analysis. Once precipitate had formed, $BaSO_4$ was extracted from filter paper via combustion and packed in tin capsules to be analyzed for sulfate isotopes and concentrations. Samples were analyzed using a continuous flow isotope ration mass spectrometer (CF-IRMS) to obtain $\delta^{34}S$ values in parts per thousand (‰) in comparison to VCDT (Vienna-Canyon Diablo Troilite). STB (-2 ‰) , and sea water (+21 ‰) standards were also packed for analysis (Krouse et., 1991). As a result of the highly pure nature of the Arctic atmosphere, with relatively low anthropogenic influences, precipitation of $BaSO_4$ often yielded little to no sulfate, which limited the extent of sulfate values in the data suite.

3.6 HYSPLIT Analysis

HYSPLIT (Hybrid Single Particle Lagrangian Integrated Trajectory) model was employed to study influences of nearby aerosol source regions on samples. The HYSPLIT model was developed by the NOAA (National Oceanic and Atmospheric Administration) to compute air parcel trajectories and deposition of atmospheric pollutants. Backwards air mass trajectories were calculated for 72 hrs. prior to sampling for air masses at 500 m, with isobaric vertical motion calculation (Stein et al., 2015).

3.7 Uncertainty and Statistics

Error bars on plots showing concentration of ice nucleating particles at a given temperature (INP(T) (L^{-1})) were not included on graphics in order to improve the visibility of the data within the plot. Error bars in the x direction (Freezing temperature) were ± 0.5 ^{o}C. Error for the y dirrection utilized statistical uncertainty for ice nucleation events after Koop et al., (1997). Partial derivitive error propagation and standard deviation were considered for uncertanties in this study. Comparisons for significant differences between samples was conducted using a one-tailed t-test, with a 95% confidence limit for significance . T-tests between the slopes of the ice nucleating particle concentrations (L^{-1}) and freezing temperature (^{o}C) were used to identify commonalities in ice nucleating characteristics. As the particles were being cooled, all slopes in this analysis have negative values.

Chapter Four: Ice Nucleation Concentrations and Isotope Results

4.1 Filtered vs. Unfiltered samples

Larger particulate matter (> 0.40 µm) was expected to not display significant influence on INP(T) values, following similar methodology (Wilson et al., 2015; Irish et al., 2018). Ice nucleation results for filtered (0.40 µm pore size) vs unfiltered samples were explored in order to confirm that larger particulate matter did not, in fact, have an influence on ice nucleation. This was tested using a unique sample from the 2013 Calgary large scale precipitation event which caused significant urban and rural flooding in Bow River watershed. As a result of multiple consecutive days of rain in June 2013, much of the urban aerosol presence was expected to be washed out, thus giving a very clear samples representative of the precipitation alone. The data shown in Figure 4-1a shows distinct clustering in three groups. The first group between 0 to 0.5 million ice nucleating particles (L^{-1}) the unfiltered/filtered samples follow the 1:1 line, indicating there is no loss or gain of ice nuclei due to filtration. However, above 5×10^5 L^{-1}, the concentration of ice nucleating particles is higher for filtered samples. This suggests that the filter could be contributing to in the INP population of the sample. The final point lies below the 1:1 line, more consistent with reduced INP concentrations after the filtration process.

Unfiltered and filtered samples were also compared via frozen fraction (Figure 4-1b), where the fraction of frozen droplets is plotted for both samples. As frozen fraction represents the percentage and cumulative rate at which droplets are frozen. If the samples fall along a 1:1 line, it represents similar rates of freezing between the filtered and unfiltered samples. As indicated in Figure 4-1b, the data falls well within error of a linear fit, demonstrating consistent rates of freezing

for both the unfiltered and filtered samples, and low effects from the filtration process. As a result of the linear relationship, it is likely that ice nucleation is dominated by smaller particles in the region < 0.40 μm.

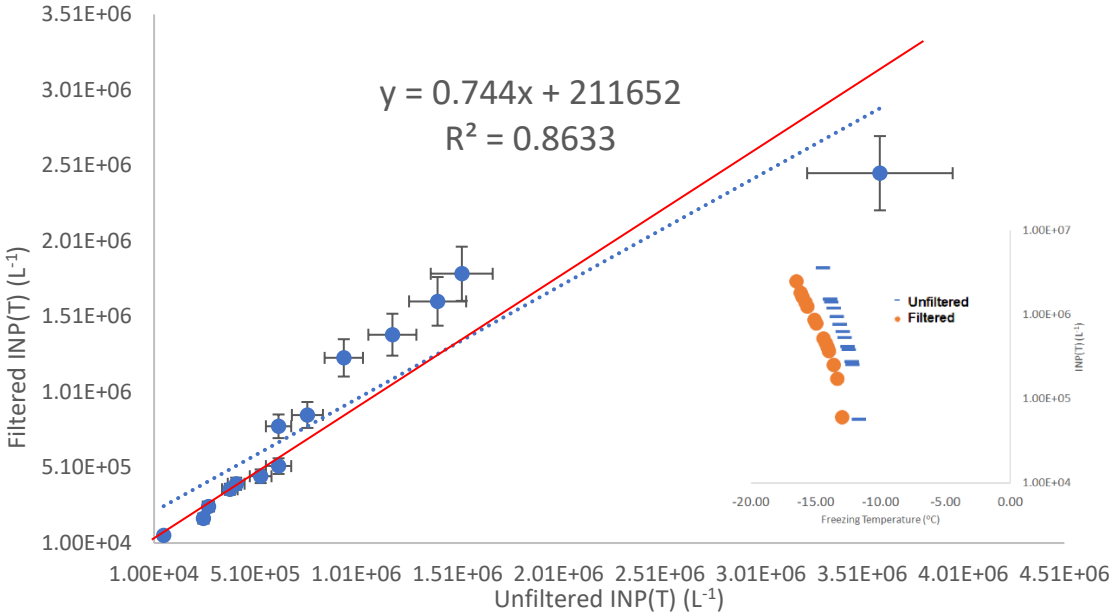

a)

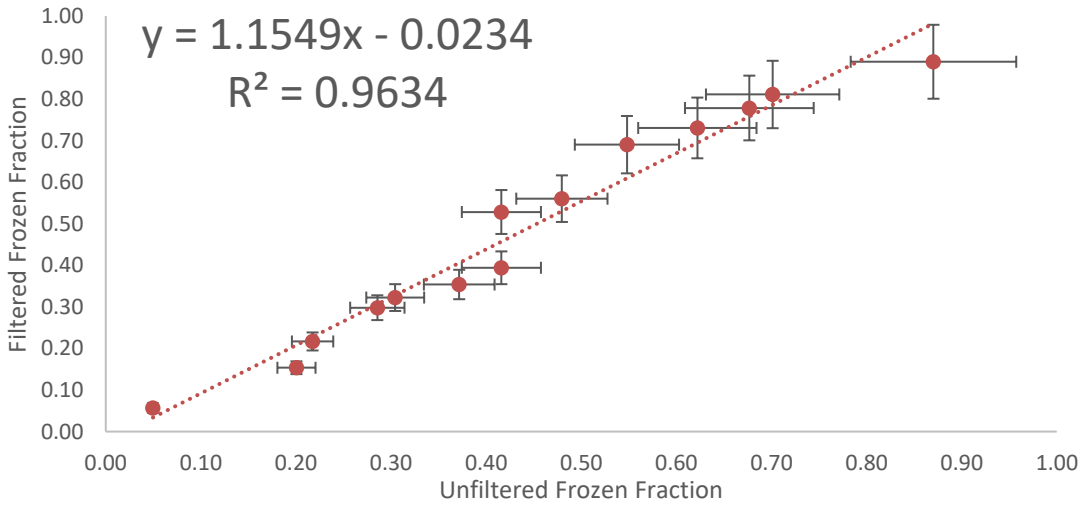

b)

Figure 4-1 Comparison of ice nucleating particle concentrations of unfiltered samples vs filtered samples (a). The dashed line represents the linear fit, while the solid line indicates a 1:1 relationship. The overlaid image shows the ice nucleation concentration (L^{-1}) with respect to freezing temperatures for reference. Fraction of total frozen droplets is shown in (b). Samples for this test were from the 2013 Calgary floods. Comparison to a 1:1-line fit is shown.

4.2 Precipitation Blanks and Samples

Comparisons of blanks and samples for 2016 were considered. Blanks were created by passing deionized distilled water through the sampler after a rinsing procedure. Figure 4-2 shows a comparison of the blanks and samples for the two samplers used onboard the ship. For the more traditional deposition rain sampler (VW), the blanks show freezing is initiated at a lower temperature (roughly 3 ^{o}C), than that of the sample, with linear cooling following initial ice nucleation. The second sampler (EC) showed similar linear trends in ice nucleation. Unexpectedly there was some discontinuity in blanks and samples between the two samplers, with both a sample and a blank in the EC sampler initiating ice nucleation at the same temperature. Furthermore, one of the blanks for the EC sampler presented clearly warmer freezing temperatures than its counterpart sample for the entirety of the frozen fraction. It is possible that these samples could have been influenced by major aerosol source regions in the Arctic, such as the Smoking Hills (Rempillo et al., 2011). Backward airmass trajectories for the 72 hour period prior to sampling are shown and are discussed in Section 5.2 below).

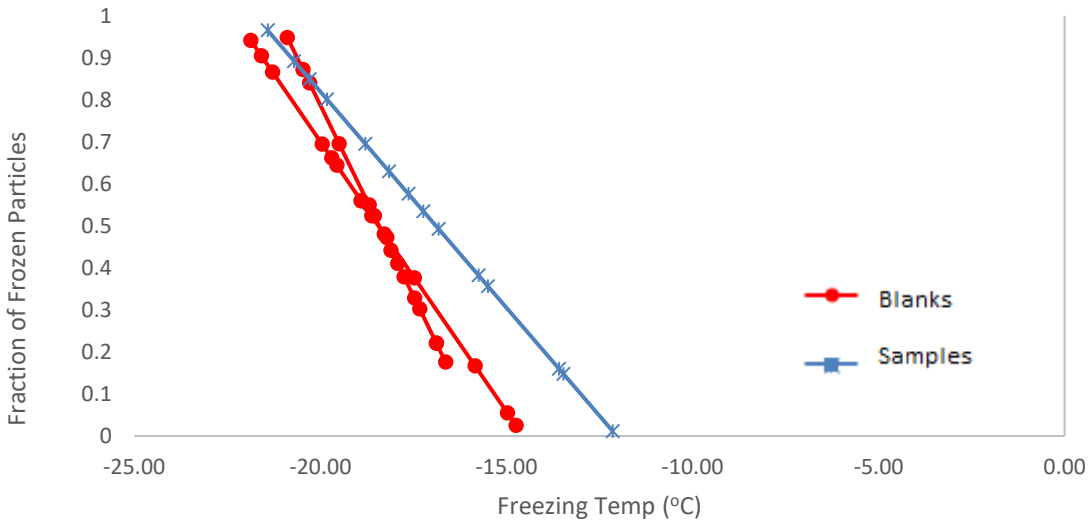

a)

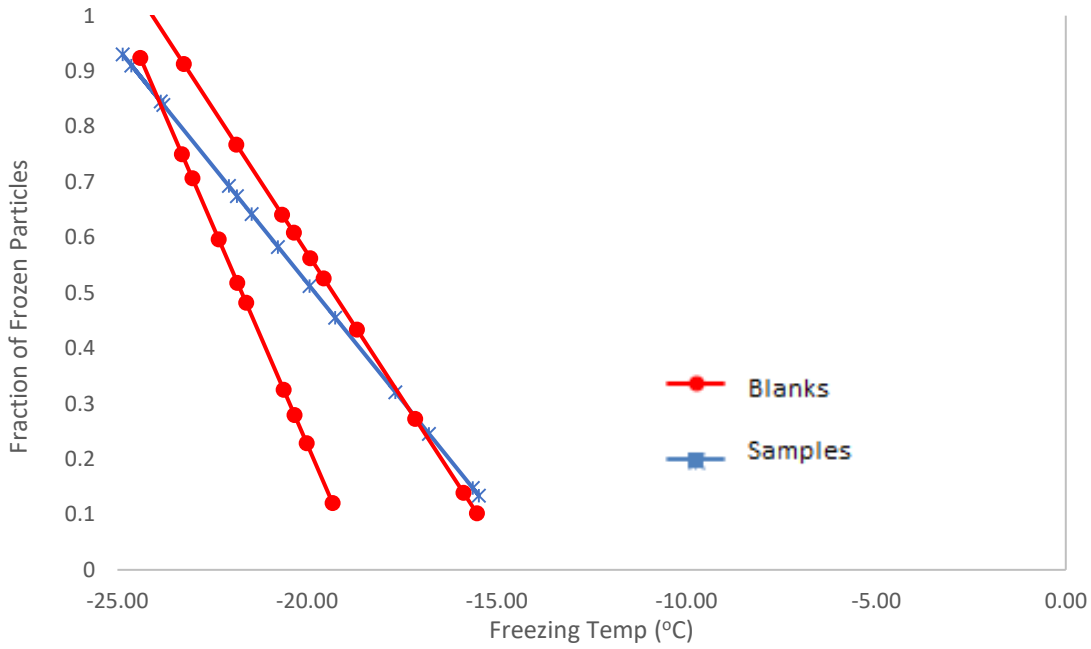

b)

Figure 4-2 Comparisons of blanks (red) and samples (blue) for Arctic samples taken on August 23rd, 2016. Measurements were divided by the type of sampler used. Environment Canada (EC) sampler (a) and a passive rain collector (VW) (b).

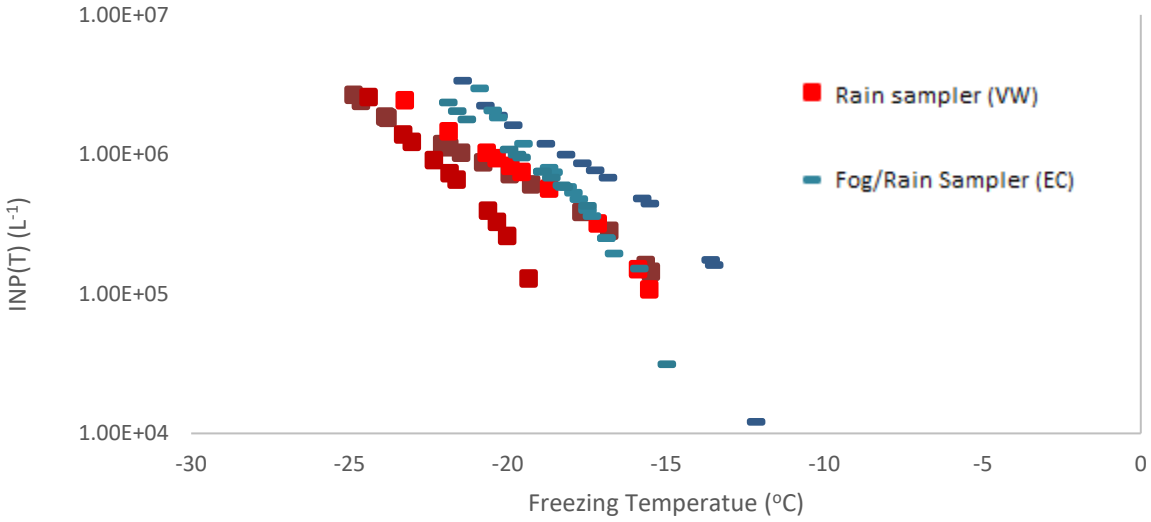

Figure 4-3 Sampler comparisons of INP(T) values for two different samplers for dry deposition samples taken on August 23rd, 2016. Traditional rain sampler (VW) is shown with red boxes, while the rain/fog (EC) sampler is shown in blue lines.

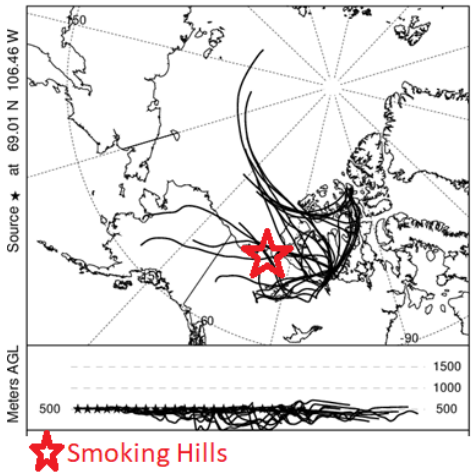

Figure 4-4 HYSPLIT backward air trajectory for August 23rd sampling location. Duration of the trajectory was for 72 hours prior to sampling, at 500 m above ground level.

4.3 2014 versus 2016 Arctic Samples

4.3.1 Ion/Cation Results: Arctic 2016

The variability in ion and cation concentrations were analyzed for the Arctic 2016 samples. Several samples presented significantly different concentrations in comparison to the bulk of the samples. For the sampling days with higher concentrations back trajectories (Figure 4-6) were calculated in order to search for influences from regional aerosol sources in the Arctic. However, these air mass trajectories did not indicate any influence from known nearby sources. Panels a), b), and c) air trajectories in Figure 4-6 all contained air masses from the Canadian Arctic Archipelago, with no air masses coming from anthropogenic sources or the Smoking Hills.

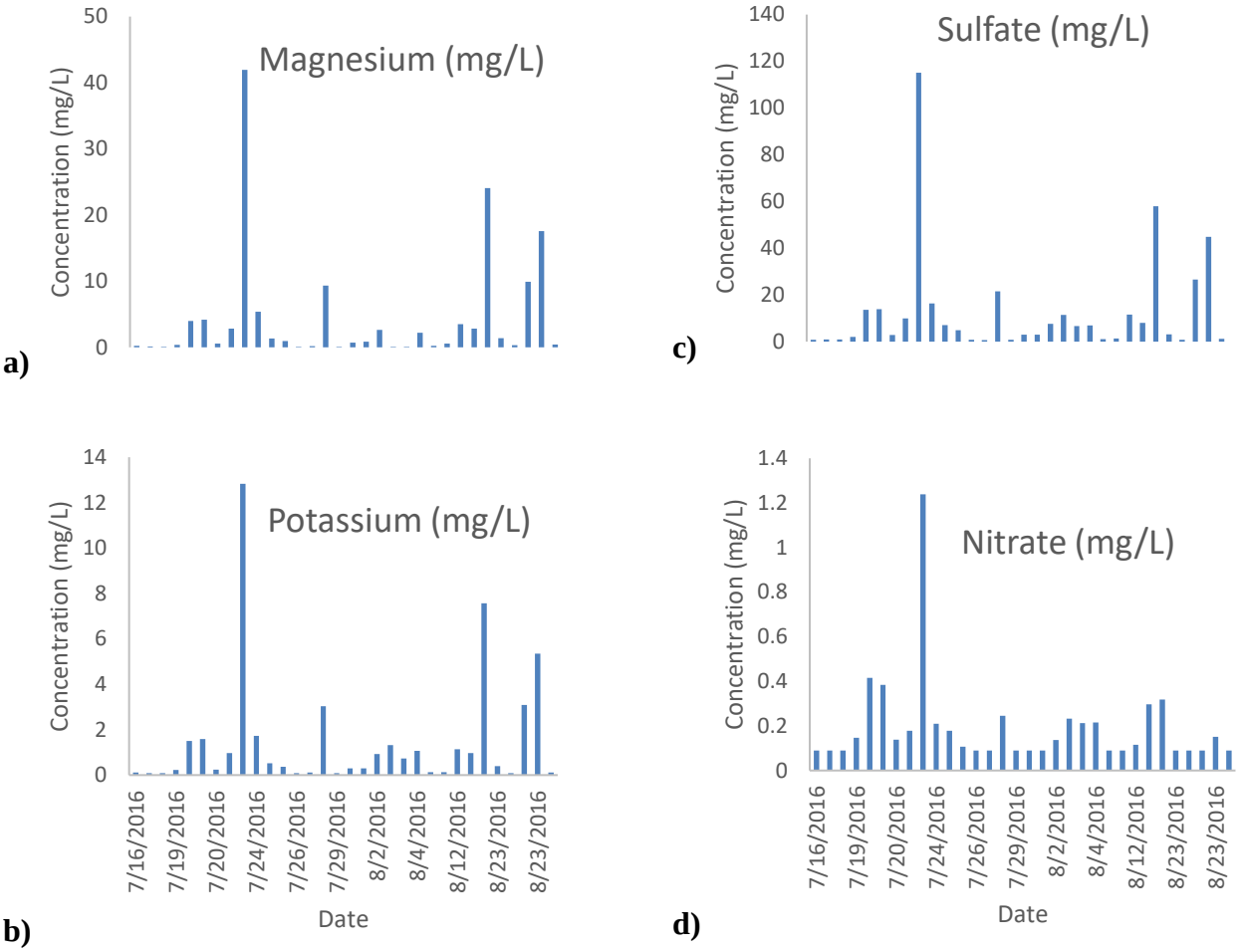

Figure 4-5 Ion/Cation analysis for 2016 Arctic samples. Concentrations of Magnesium (a), Potassium (b), Sulfate (c), and Nitrate (d) all pointed to specific sampling days with significantly higher ion/cation concentrations than the bulk of the samples (July 18, July 23, Aug 23). Air mass back trajectories were calculated for these days to observe any influence of known sources.

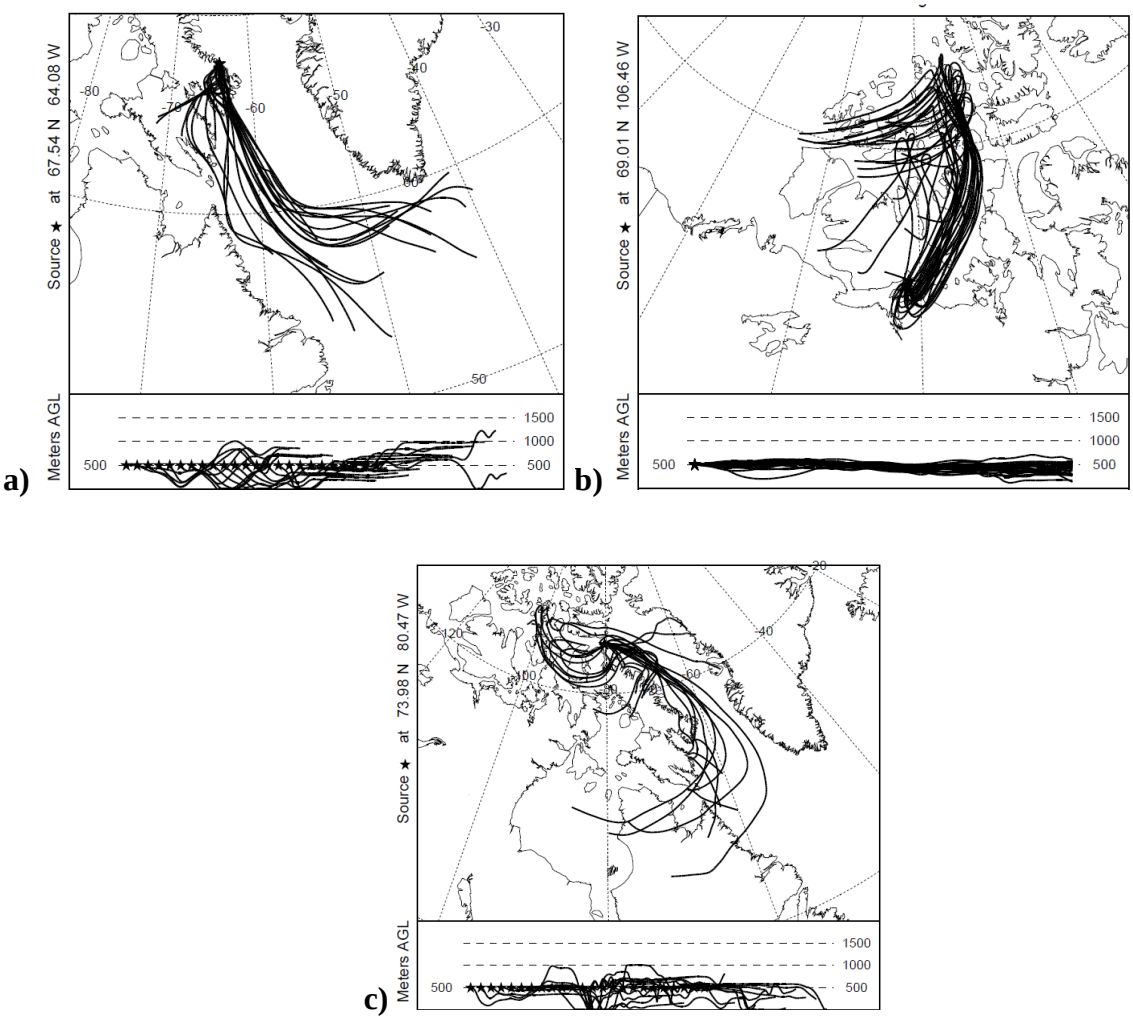

Figure 4-6 Back trajectories for July 27, 2016 (a), July 23 (b), and August 23rd (c) calculated for 72 hours prior to the sampling date.

4.3.2 INP Concentrations: 2014, 2016 Fog +Rain

Precipitation samples were taken in the Arctic for summer research voyages aboard the *Amundsen* during both 2014 and 2016. The ice nucleation properties of these samples were measured using the droplet freezing technique described in Section 3.3. The minimum-maximum

values of these trials are shown below in Figures 4-7 and 4-8. Due to inconsistent precipitation events and a short study duration, observations of temporal variations are somewhat limited.

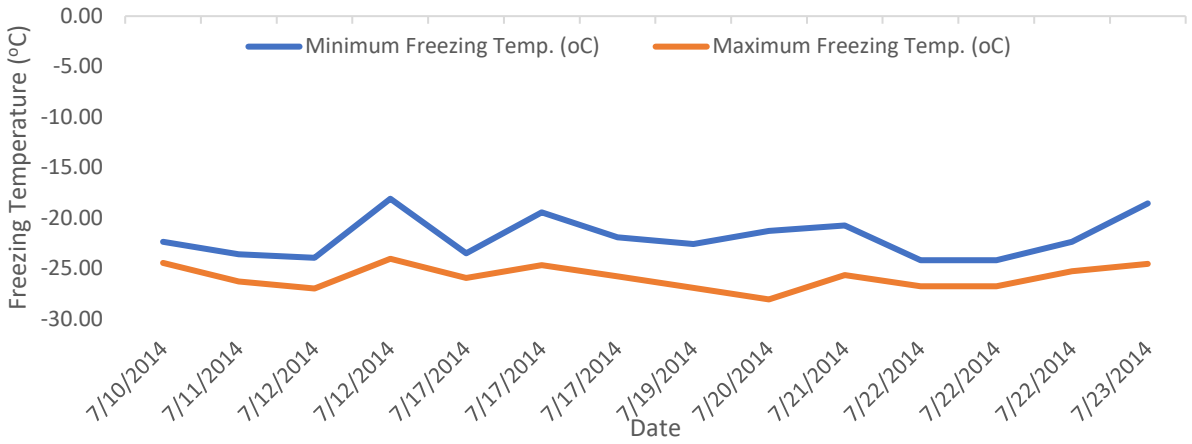

Figure 4-7 Ice nucleation minimum/maximum freezing temperatures (ºC) for the Arctic 2014 dataset. Multiple days are representative of AM/PM samples and multiple precipitation events in a single day.

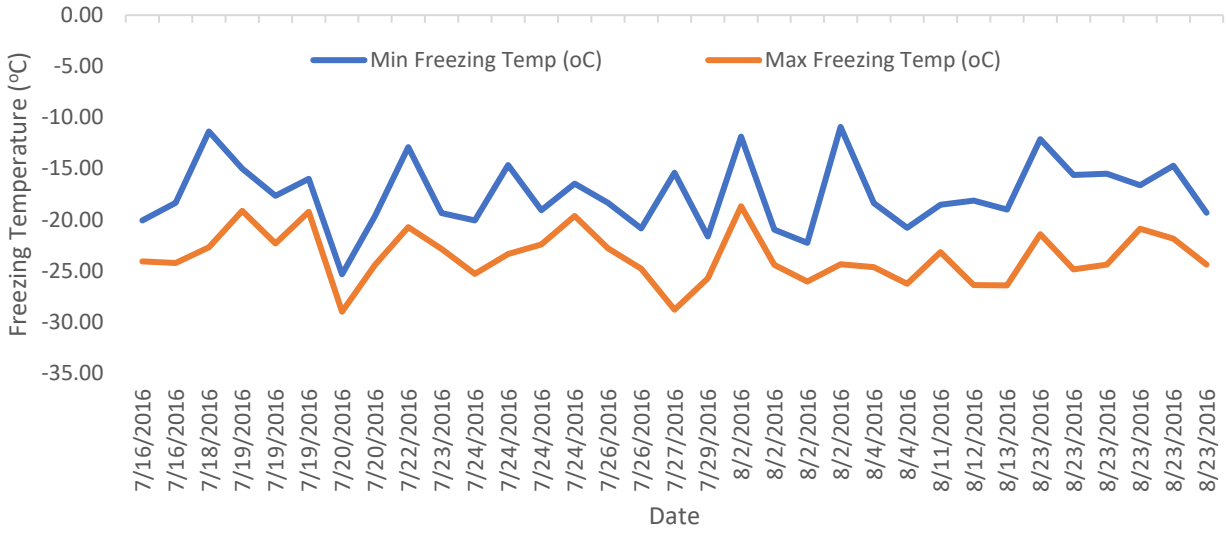

Figure 4-8 Ice nucleation minimum/maximum freezing temperatures (ºC) for the Arctic 2016 dataset. Multiple days are representative of AM/PM samples and multiple precipitation events in a single day.

Fog and rain data over 2014 and 2016 were separately compared to see if there were differences over the two years (Figure 4-9;4-10). While the 2016 rain data presented clearly warmer freezing temperatures ranging from -10 to -25 ºC, the 2014 data yielded cooler freezing temperatures ranging from -18 to -28 ºC (Figure 4-9). Similar comparisons were done with the fog data from both years (Fig 21), where 2016 data ranged from -15 ºC to -25 ºC, and 2014 data ranged from -18 ºC to -27 ºC.

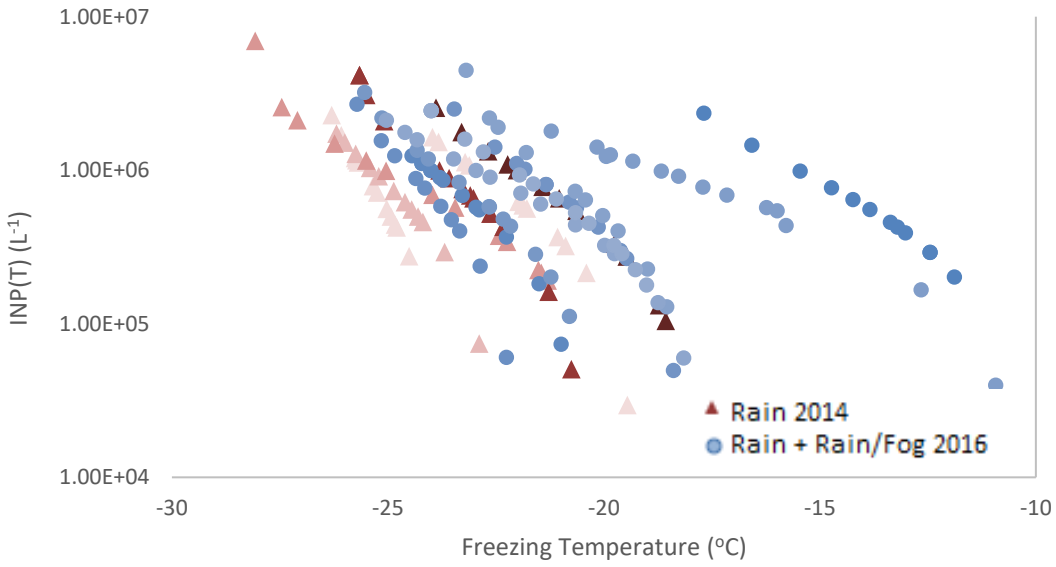

Figure 4-9 INP(T) values comparing 2014 to 2016 precipitation for rain samples.

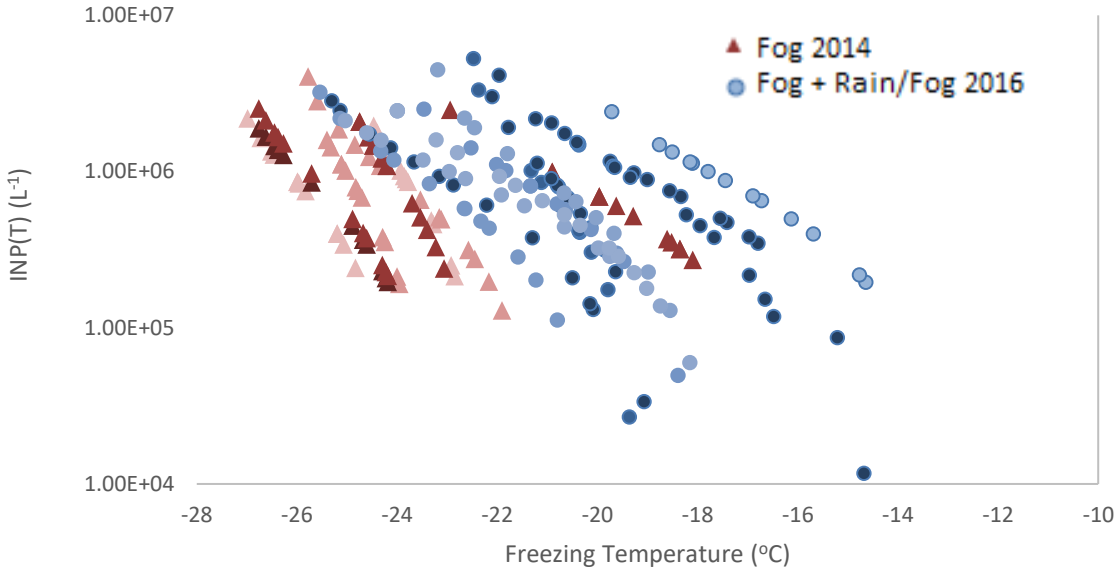

Figure 4-10 INP(T) values comparing 2014 to 2016 precipitation for fog samples.

In order to further explore the interesting behavior exhibited in the blank samples from the August 2016 precipitation data, specific results from the two samplers were compared in order to observe any systematic differences that might arise as a result of a sampling bias. The dry deposition results did not display any clear grouping, although IN data from the rain (VW) sampler have shallower slopes and warmer IN temperatures ranging from -13 °C to -25 °C, whereas the fog (EC) sampler displayed steeper IN slopes and cooler IN temperatures ranging from -13 °C to -27 °C (Figure 4-11).

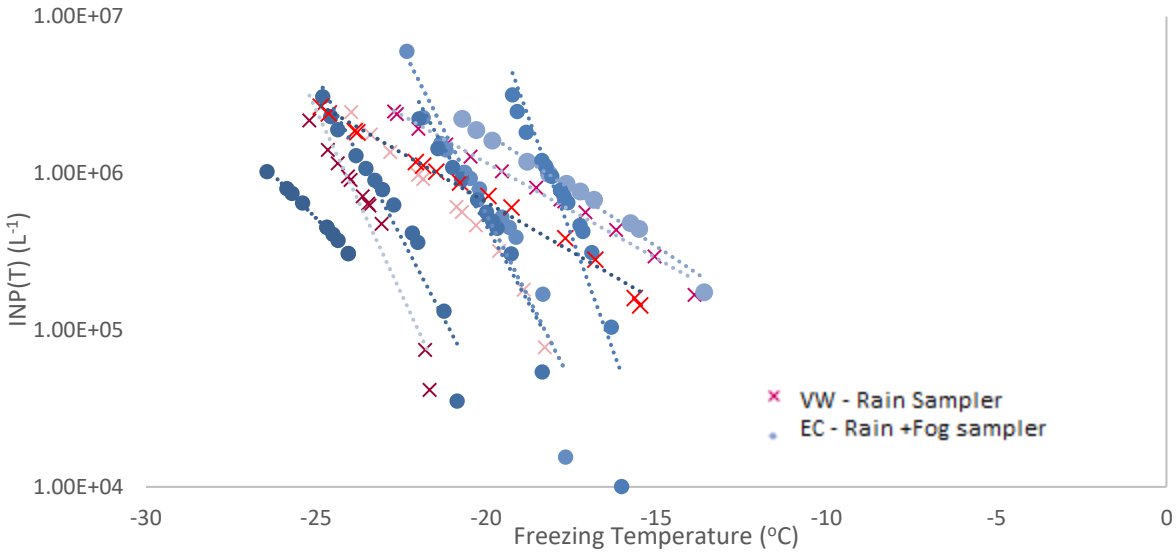

Figure 4-11 Different samplers for 2016 Arctic dry deposition data. EC sampler is marked with circles and VW sampler is marked with crosses.

4.4 Rural and Urban Continental Samples

4.4.1 Ion/Cation Results

Ion cation analysis was performed on the Kananaskis/Calgary samples, with two dates (Jan 6th, and 9th) appearing to display unusually high concentrations of both magnesium, sulfate, and calcium (Figure 4-12).

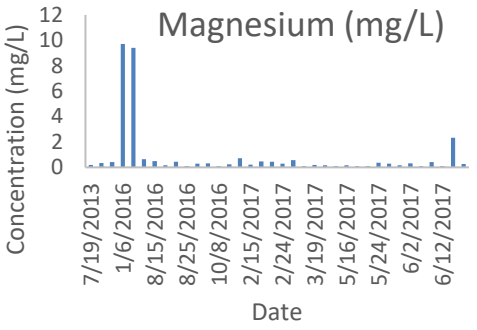

a)

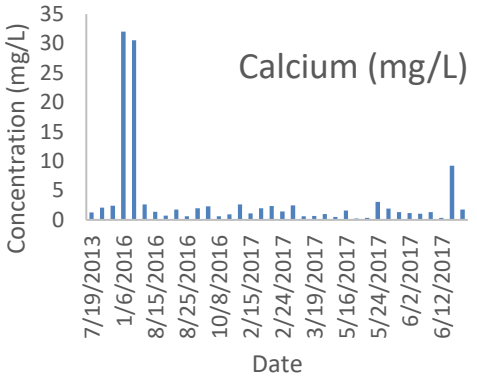

c)

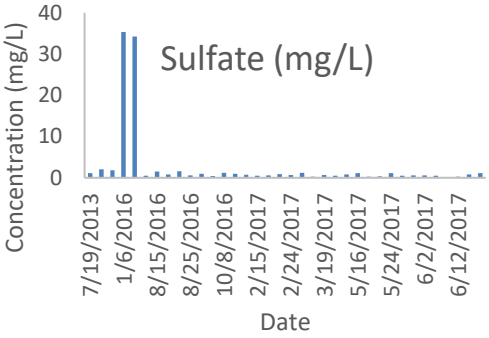

b)

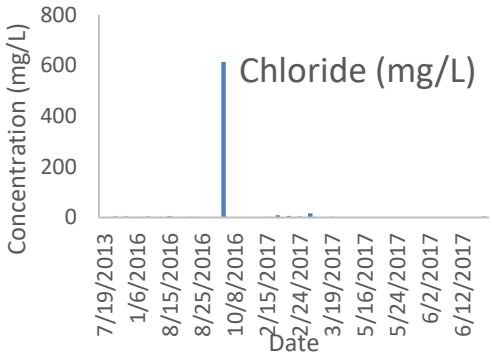

d)

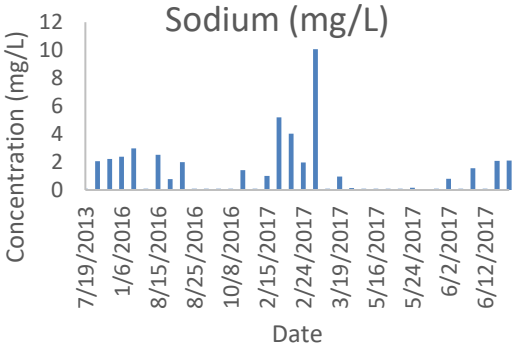

e)

Figure 4-12 Ion/Cation analysis for the Kananaskis and Calgary Data. Magnesium (a) sulfate (b) calcium (c) Chloride (d) all showed extremely high concentrations for Jan 9th and Jan 6th. Sodium concentrations used for sea salt contributions calculations are shown in e) Precipitation records noted low visibility and high fog on Jan 6th, whereas Jan 9th had ice crystals present in the early morning.

4.4.2 Kananaskis/Calgary Air Mass Back Trajectories

Further HYSPLIT analysis was conducted based on both ion/cation and ice nucleation data from the Calgary/Kananaskis data sets. For ion cation data, sites which showed concentrations ~ ten times greater than average anion/cation results (Figure 4-12) were chosen. Additionally, from ice nucleation data, samples from respective groupings (rain, fog, dd) which displayed characteristics atypical compared to the bulk of the remainder of the sample grouping were also selected. Based on this criteria winter Calgary Jan 3rd;6th;9th (Figure 4-13), Kananaskis winter/spring samples from Feb 22nd, and May 24th (Figure 4-14), and a Calgary summer sample from June 14th (Figure 4-15) were chosen for HYSPLIT analysis.

January 3rd trajectories contained air mass influences from both Pacific 2 and local air mass sources (Ge et al., 2016; Stenhouse et al., 2016). January 6th contained air mass influences from both the pacific and local sources. It is possible that the back trajectories contained some influence from the Arctic source region. The January 9th sample from Calgary contained air mass influences from the NE continental source, with no influence from marine or Arctic sources. Calgary samples from June 14 contained air mass influences from Pacific 2,3,4 and local regions.

The trajectories from Feb 22nd (Kananaskis sample) was influenced by air masses from Local, Pacific 4, and South Pacific source regions. May 17th contained air mass trajectories from Pacific 2,3, and 4 in addition to local influences.

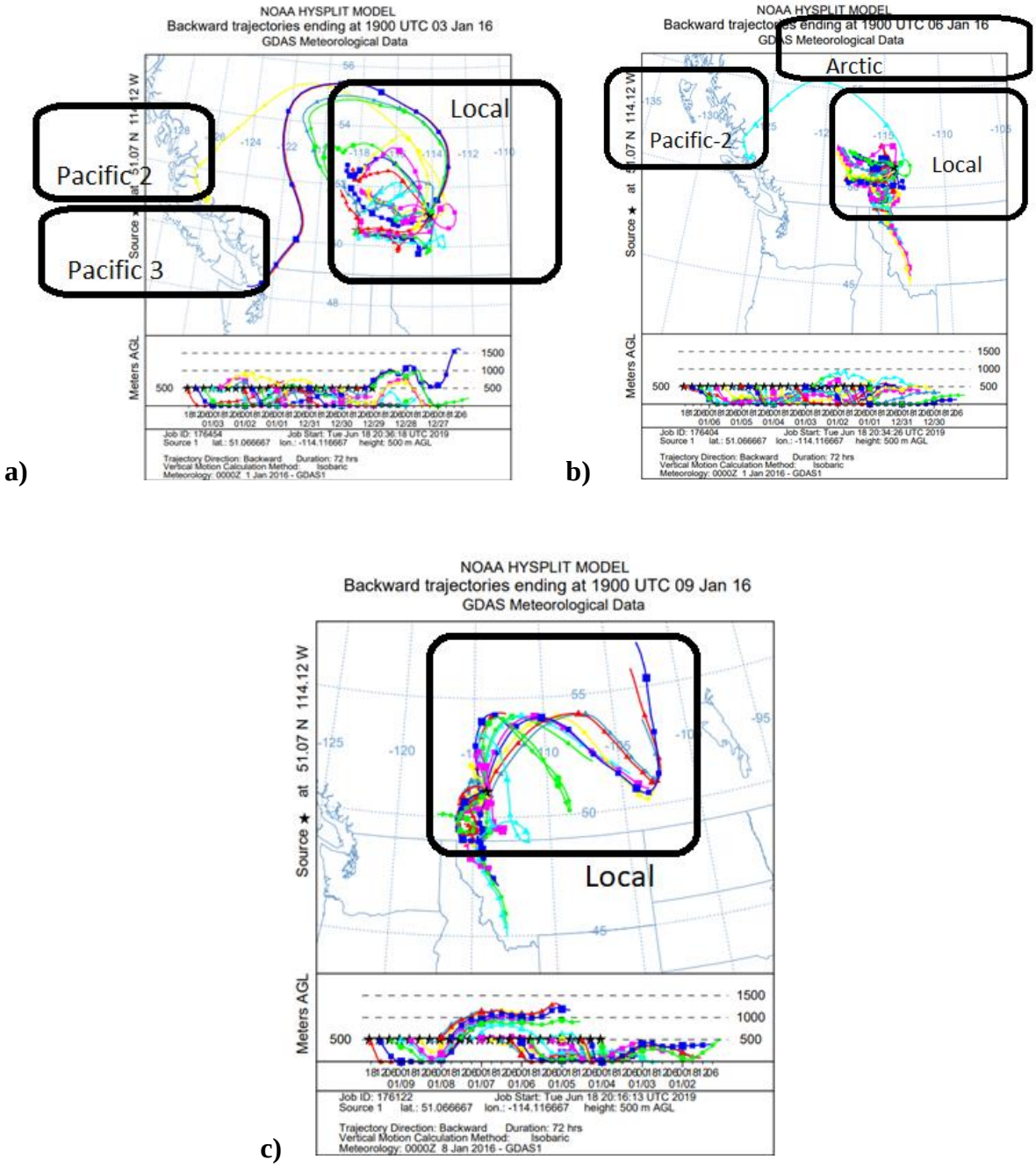

Figure 4-13 HYSPLIT model back trajectories for Calgary winter 2016 samples Jan 3rd (a), 6th (b), and 9th (c) respectively. North American air masses are also shown overtop of the trajectory pathways.

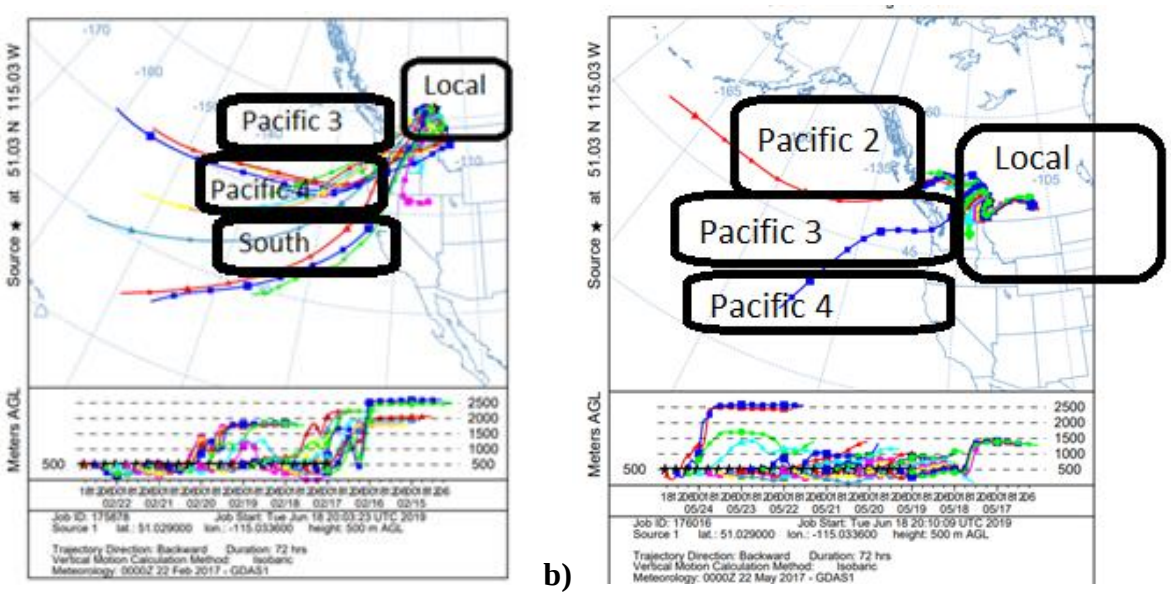

a) b)

Figure 4-14 HYSPLIT model back trajectories for Kananaskis 2017 samples for Feb 22nd (a), and May 24th (b). North American air masses are also shown overtop of the trajectory pathways.

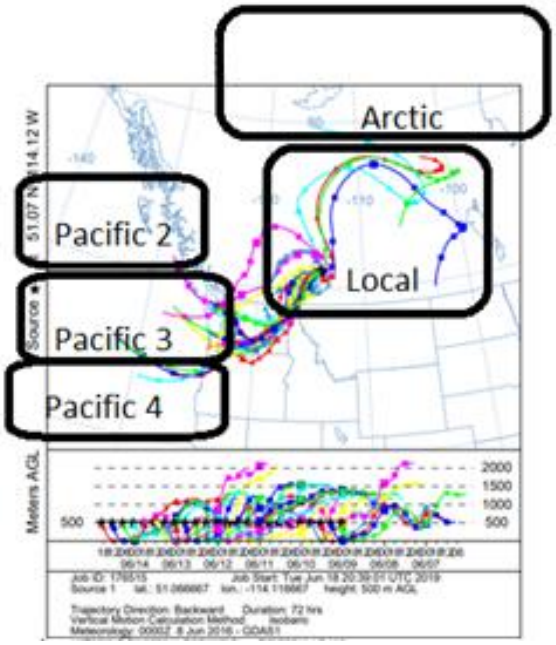

Figure 4-15 HYSPLIT model back trajectories for Calgary 2016 summer sample from June 14th. North American air masses are also shown overtop of the trajectory pathways.

4.4.3 INP Concentrations: Urban and Rural Continental

Precipitation samples were taken in the urban (Calgary) and rural (Kananaskis) continental study sites. The ice nucleation properties of these samples were measured using the droplet freezing technique described in Section 3.3. The minimum-maximum values of these trials are shown below in Figure 4-16 and 4-17. Sampling was limited to larger precipitation events, and thus observations of temporal patterns were limited as a result of gaps between sampling dates.

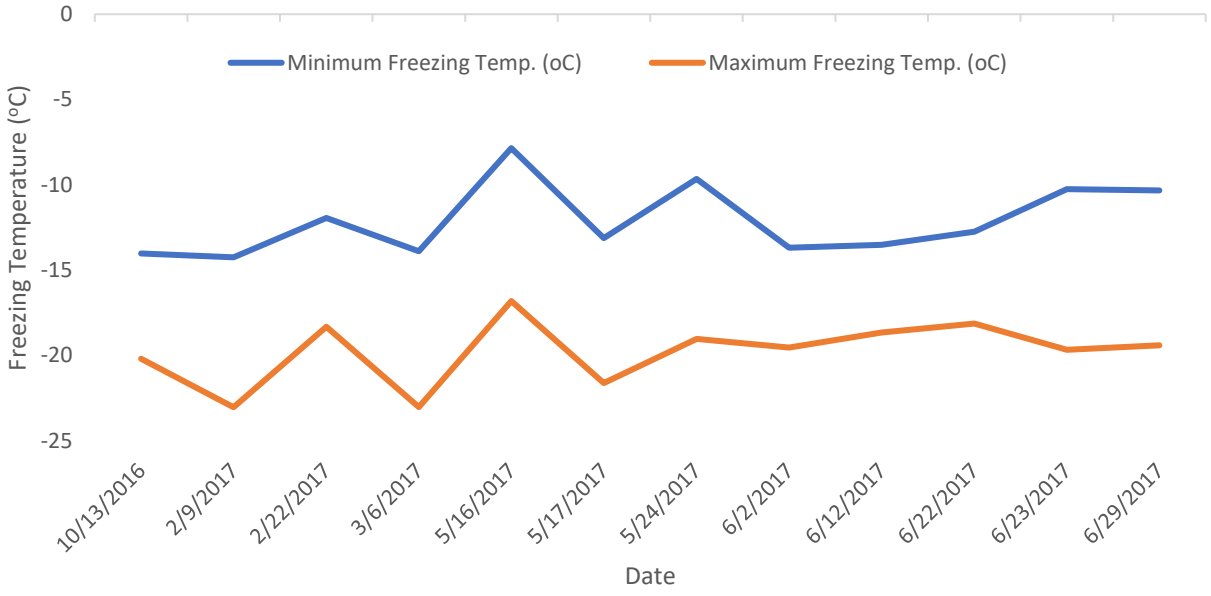

Figure 4-16 Ice nucleation minimum/maximum freezing temperatures (°C) for the Kananaskis sample suite.

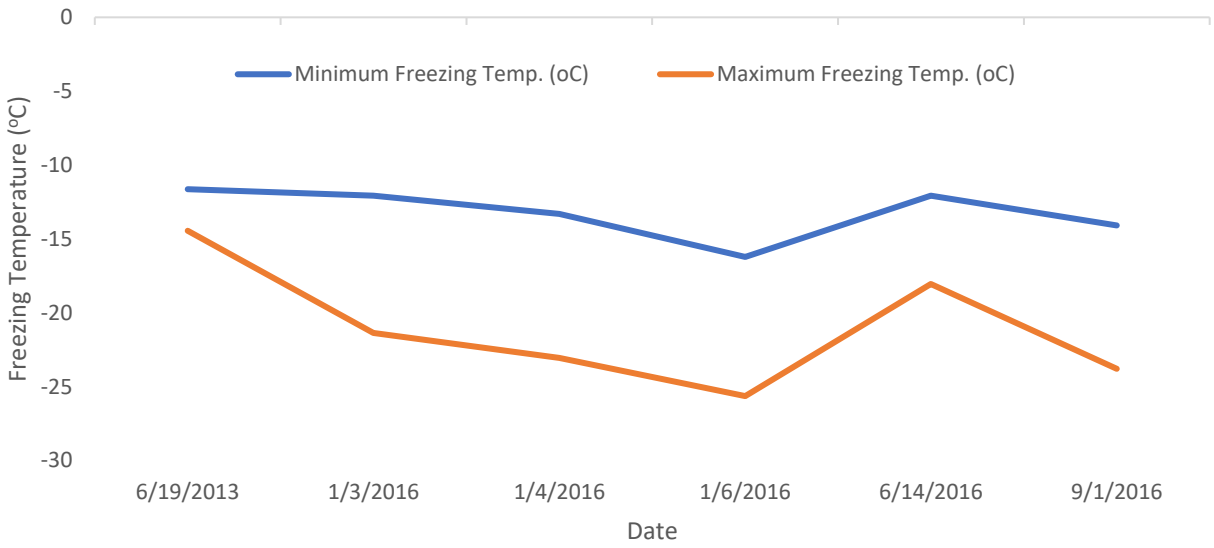

Figure 4-17 Ice nucleation minimum/maximum freezing temperatures (ºC) for the Calgary sample suite.

A difference between ice nucleating concentrations of rain and snow samples was also observed. A clear distinction between most of the rain and snow samples is present in Figure 4-18, with a distinct clustering of rain and snow samples excluding two samples. A late snow sample from May 24th displayed INP(T) pattern closer to rain samples with the daily temperature of 1ºC to 10 ºC, while the sample was recorded as 6.6 cm of snow. Additionally, a Feb 22nd sample was also outside the normative value for snow samples and exhibited INP(T) patterns observed in the remainder of the rain samples. Temperatures for Feb 22, 2017 ranged from -4 to -9 ºC with 10.2 cm of snow recorded, Feb samples listed as rain were clearly in line with the rest of the snow samples. The same pattern was seen for precipitation samples where May samples listed as snow lined up with the values in precipitation samples taken at the time.

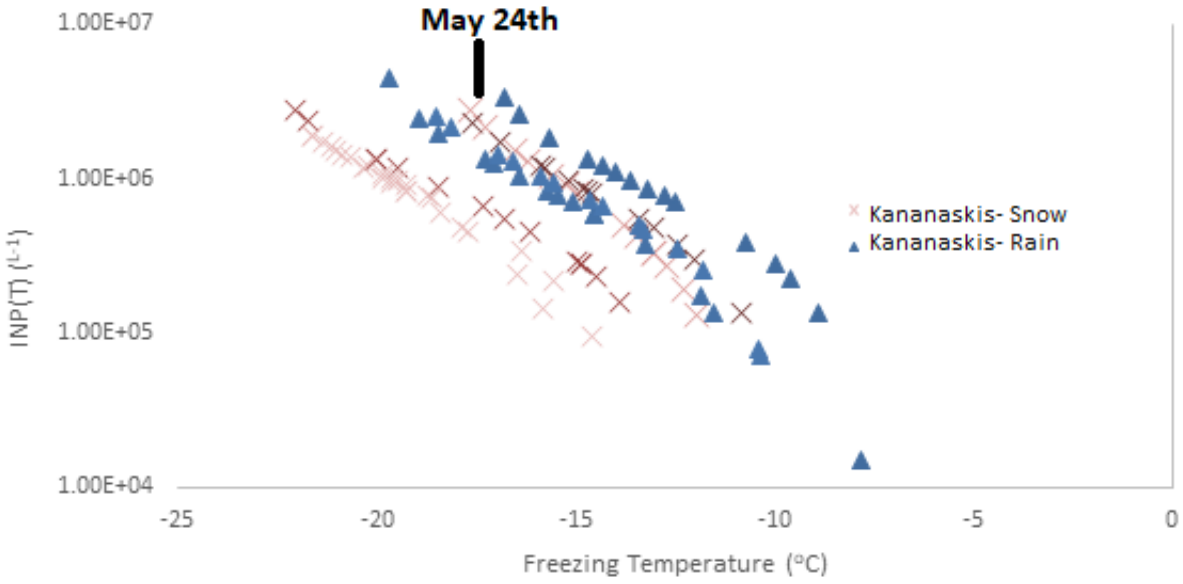

Figure 4-18 Comparison of rain (Triangles) and snow (crosses) ice nucleation particle concentrations for the Kananaskis region for 2017.

Calgary and Kananaskis dry deposition were compared and clear differences were observed between the urban and rural samples (Figure 4-19). The Calgary dry deposition samples had much shallower freezing curves, while the Kananaskis samples freezing curves appeared to be steeper. Furthermore, the dry deposition and precipitation sampling in Calgary (Figure 4-20) demonstrated differences in IN for the urban environment. In general, Calgary precipitation and dry deposition contained shallower slopes but colder freezing temperatures, whereas Kananaskis dry deposition contained steeper slopes with warmer ice nucleating temperatures. Calgary January 3rd and June 14th samples demonstrated freezing temperature ranges and curves much closer to the rural Kananaskis sample IN curves (Figure 4-20).

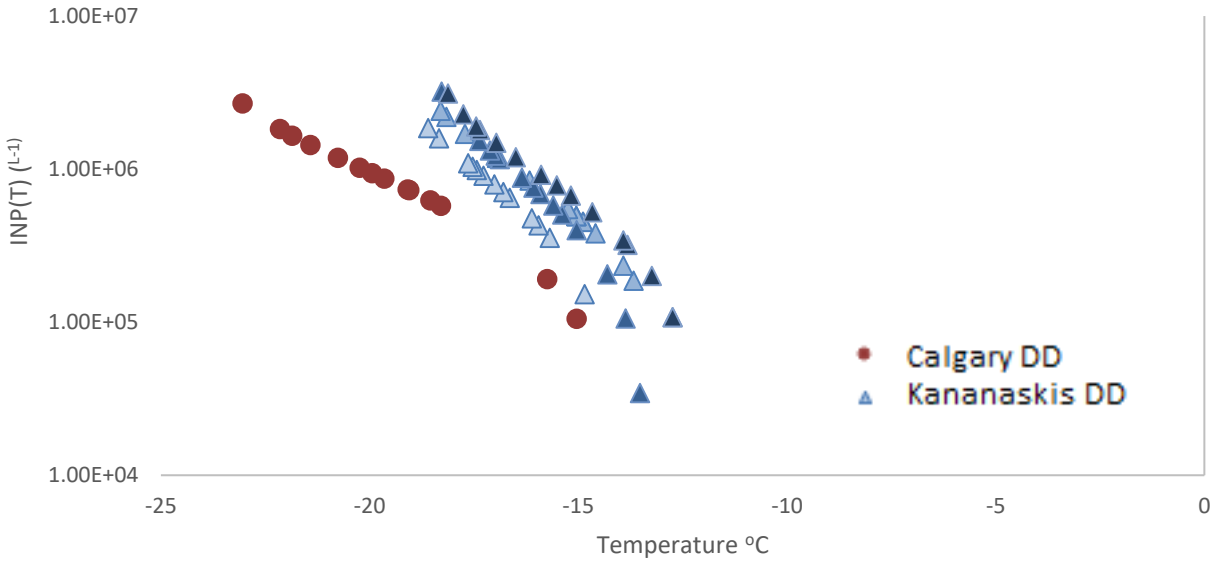

Figure 4-19 Comparison of Calgary (red circles, representing a cumulative multi day sample) and Kananaskis (blue triangle) dry deposition sampling.

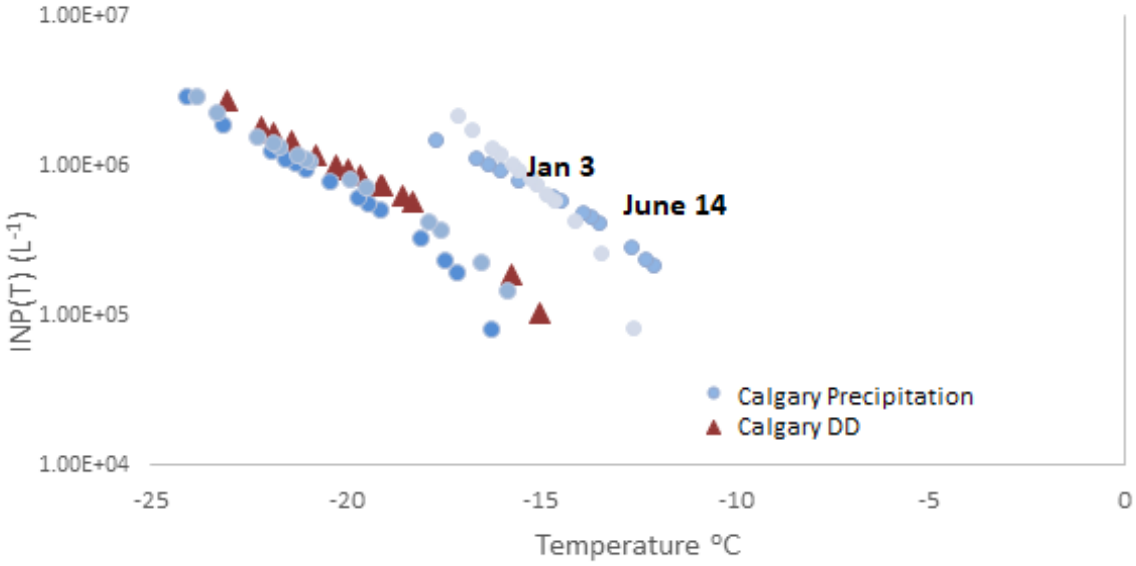

Figure 4-20 INP(T) concentrations for Calgary dry deposition and precipitation samples for 2016 samples.

4.5 Sulfur Isotope Results

In order to define the sources of sulfate within the precipitation samples, known isotope values (δ^{34} S) were compared to the isotope results from the regional precipitation samples. The δ^{34} S values versus the percentage of sea salt sulfate for Arctic and Calgary/Kananaskis is shown in Figure 4-21a, b, respectively. Samples consistently lined up within the mixing lines for sea salt and the appropriate end members for continental and Arctic locations respectively. Sea salt/sour gas and sea salt/vehicle exhaust mixing lines are shown for continental Alberta samples (Figure 4-21a). Sea salt/biogenic sulfate and sea salt/anthropogenic sulfate mixing lines are shown for the Arctic samples (Figure 4-21b). The Kananaskis samples were mainly consistent with influences from anthropogenic sources, with an upper end member assignment of +13‰, appropriate for well mixed air from oil and gas and vehicle exhaust. The lower end member of +5‰ is consistent with vehicle exhaust, indicating contributions from this source for many of the samples. The single sample outside the dashed mixing line for June 22, 2017 in the Kananaskis in Figure 4-21a has an endmember more consistent with lithospheric sulfate influences (or non-marine biogenic sulfur from nearby continental sources) at -5‰.

The δ^{34}S for the Arctic samples showed contributions from DMS with upper endmembers of +18‰, and lower endmember of +3‰ indicating well mixed air from anthropogenic, DMS, and sea salt sulfate, and is consistent with what has been described for aerosols in the literature previously (Ghahremaninezhad et al., 2017).

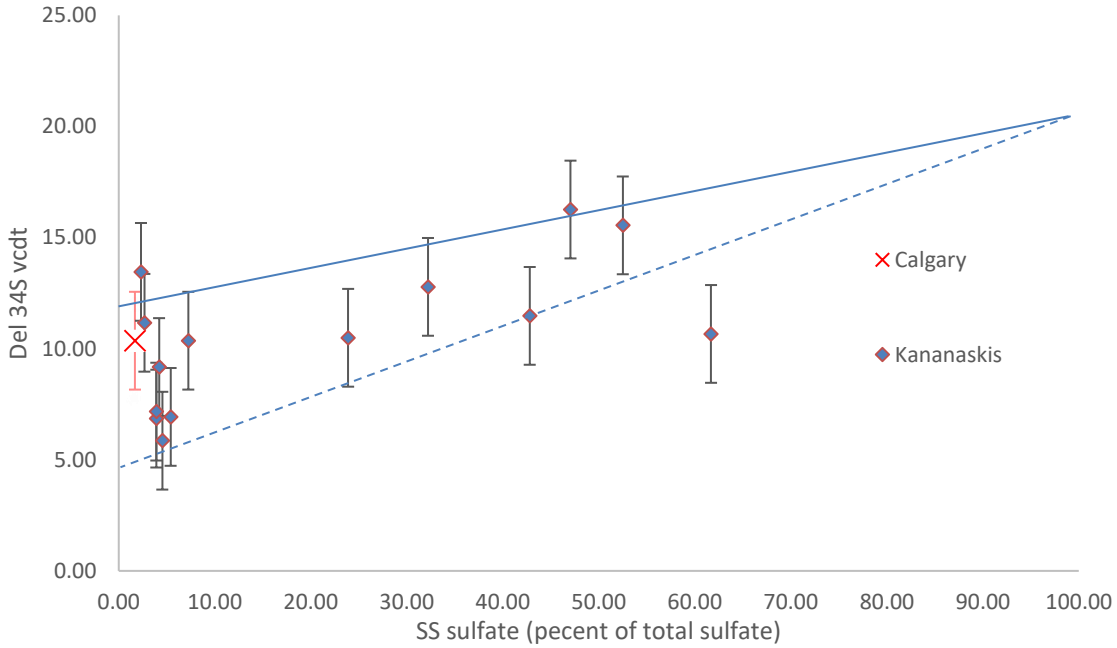

a)

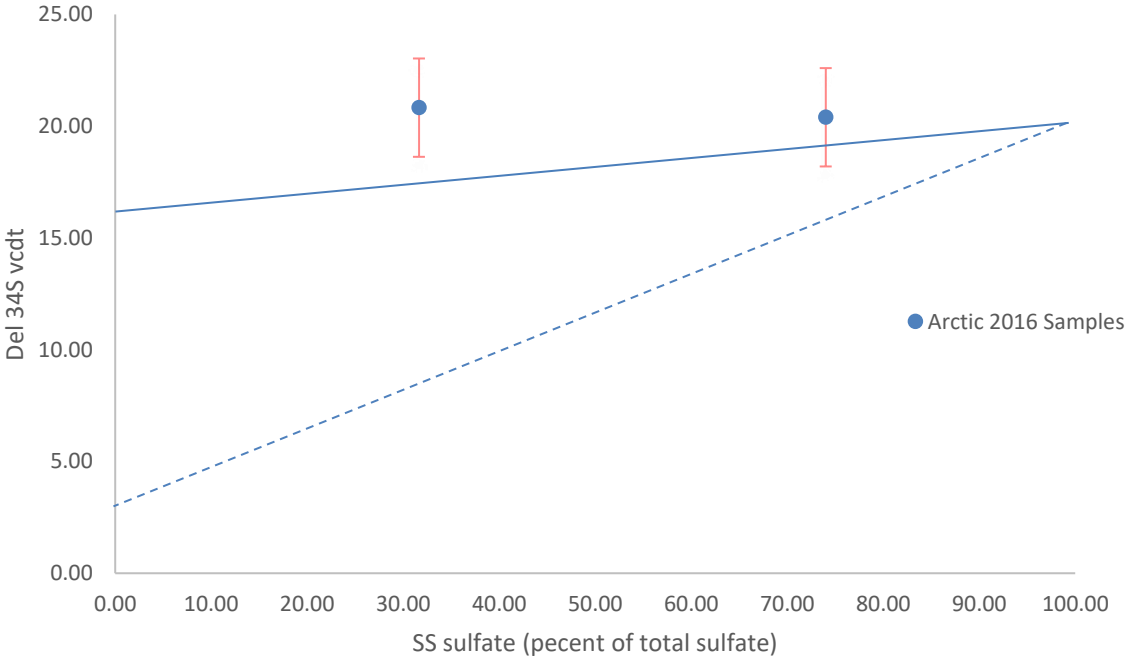

b)

Figure 4-21 The δ^{34} S values versus the percentage of sea salt sulfate for Kananaskis/Calgary samples (a) and the Arctic samples (b) are shown.

Chapter Five: Discussion

5.1 Comparison of Filtered and Unfiltered INP

The comparisons of filtered and unfiltered samples demonstrated a slight deviation from a 1:1 relationship. Dominant ice nucleation particle sizes typically exist with diameters $0.1 < d < 1$ µm (Vali, 1966), and samples were filtered with 0.40 µm filters. Figure 4-1 indicates that there were slight variations from the 1:1 line, with higher INP concentrations in filtered samples above 0.6 million L^{-1}. With IN particle concentrations (L-1) from 0 to 0.6 million, the ice nucleation process follows the 1:1 line, leading to the indication that there is no loss or gain of ice nucleating particles during the initial nucleation for the first 40% of the frozen fraction of particles. For the remaining 60% of the frozen fraction (after 0.6 million L-1) the filtered samples presented lower INP(T) values as compared to the unfiltered samples. Samples following a 1:1 line, suggest that the ice nucleation process is dominated by smaller particles, and there are no large (> 0.40 µm) ice nucleating particles. Data points that reside above a 1:1 line indicate that the filter has contributed to the ice nucleating process, and the filtration process has added INP. Samples which reside below the 1:1 line indicate there is a loss of ice nucleating particles as a result of the filtration process, and that ice nucleating particles greater than 0.40 µm are present in the sample. Despite this, recent research on biogenic particles (Wilson et al., 2015) has indicated particles less than 0.2 µm are most influential in ice nucleation particles, suggesting that small biogenic exudates are important ice nucleating particles in marine environments. With this study's primary focus on biogenic sources (and thereby particles < 0.2 µm), the differences between filtered/unfiltered samples do not appear to be of significant relevance.

Table 5-1 Differences between filtered and unfiltered samples for a 2013 Calgary flood precipitation sample.

Unfiltered Sample		Filtered Sample		Difference in INP(T) (L^{-1}) (Unfiltered - Filtered)
Freezing Temp (^oC)	INP(T) (L^{-1})	Freezing Temp (^oC)	INP(T) (L^{-1})	
-11.63	5.70E+04	-12.93	6.02E+04	-3.20E+03
-12.15	2.54E+05	-13.34	1.72E+05	8.19E+04
-12.21	2.78E+05	-13.61	2.52E+05	2.63E+04
-12.44	3.84E+05	-13.95	3.66E+05	1.86E+04
-12.51	4.16E+05	-14.05	4.03E+05	1.32E+04
-12.74	5.37E+05	-14.19	4.52E+05	8.47E+04
-12.89	6.25E+05	-14.36	5.19E+05	1.06E+05
-12.89	6.25E+05	-14.93	7.83E+05	-1.58E+05
-13.11	7.68E+05	-15.06	8.58E+05	-9.01E+04
-13.34	9.48E+05	-15.61	1.24E+06	-2.88E+05
-13.6	1.19E+06	-15.79	1.39E+06	-2.02E+05
-13.78	1.41E+06	-15.99	1.61E+06	-1.99E+05
-13.87	1.53E+06	-16.13	1.79E+06	-2.62E+05
-14.45	3.60E+06	-16.46	2.46E+06	1.14E+06

Similar studies on snow samples in Alert, Nunavut and Barrow, Alaska also presented cooler ice nucleation temperatures for filtered samples compared with unfiltered samples (with respective mean freezing temperatures of -19.6 ± 2.4 to -8.1 ± 2.6°C), filtered with a Millex syringe filter with a 0.22 µm pore size hydrophilic PVDF membrane (Rangel-Alvarado et al., 2015). Population averages of ambient ice nuclei from filtered and unfiltered rainwater have also shown to have differences, with unfiltered rainwater samples yielding colder droplet freezing temperature ranges (-20 to -30 ^oC) compared to filtered rainwater samples (-10 to -22 ^oC) (Wright et al., 2013). Despite this, preliminary data by R. Ghahremaninezhad (2017) suggests that particles 3.0-7.2 µm are most efficient INPs.

5.2 Blanks Versus Samples

Blanks were measured in order to establish a reference baseline for the ice nucleation values. It was expected that the blanks would represent low aerosol effects and freeze at temperatures much cooler than samples that contain ice nucleating particles (Irish, 2018). The relationships shown in Figure 4-1, 4-2 show the differences between the samples and the blanks. Within the 2016 sample suite, the blanks were all taken on August 23rd, 2016. For the traditional precipitation sampler, the blanks underwent ice nucleation at a colder temperature than the samples that day, in agreement with behavior of blanks in similar studies (Irish, 2018). For the fog sampler (Figure 4-2), the blanks gave values which ended up on either side of the dry deposition samples (Figure 4-2). Lower freezing temperature for blanks versus samples indicates the presence of ice nuclei in samples.

It is possible that a strong influence from regional sulfate sources could have been present that day, leading to unexpectedly high ion concentrations (Mg^{+}, NO_3^{-}, K^{+}, and SO_4^{2-}). The nearby Smoking Hills, (a significant regional source of SO_2 with estimated emission of 0.3 kg s^{-1} (Rempillo et al., 2011)) could be a possible sulfate influence on samples on August 23rd. HYSPLIT model back trajectories were calculated for 72 hours prior to the August 23rd sampling day, and several possible trajectories originating from the Smoking Hills region were linked to the sampling event on August 23rd, which could have influenced the freezing temperatures, leading to significantly altered ice nucleating particle concentrations.

5.3 Arctic Sampling Observations

With sample suites covering both 2014 and 2016, concentration of INP's, freezing temperatures, and sampling methodology for Arctic ice nuclei were compared. For 2014 only a deposition rain collector (VW) was used to collect samples for dry deposition, rain, and fog. In 2016 both the rain collector from 2014 (VW) and a passive rain and fog collector (samples collected via impact on vertical Teflon fibers) was used (Figure 5-1). Overall, the 2016 samples exhibited warmer freezing temperatures (Figure 5-2).

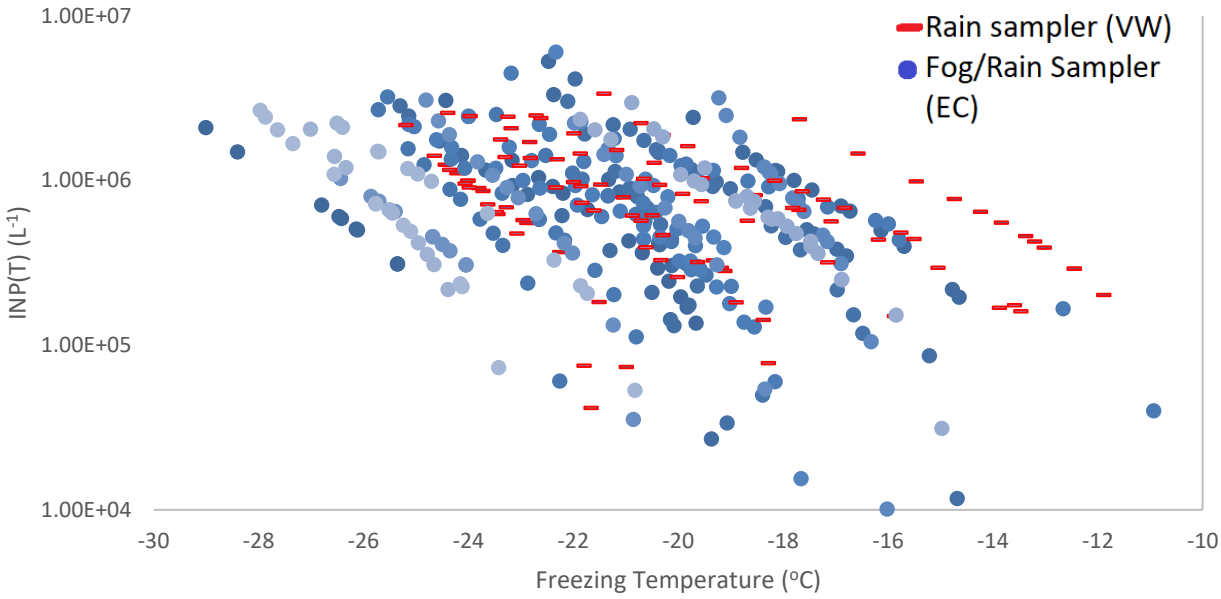

Figure 5-1 Spread of Fog/Rain samplers (Blue circles) vs Rain sampler (Red Lines) for 2016 data.

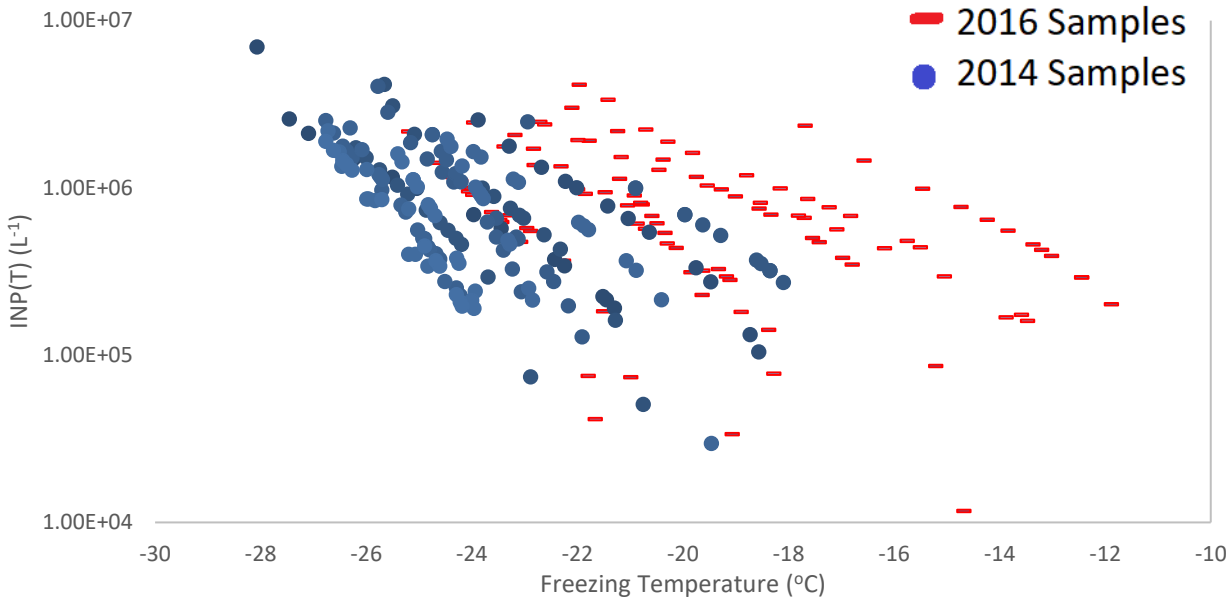

Figure 5-2 Spread of 2014 and 2016 samples taken with a passive rain sampler.

One possible explanation for the differences between the 2014 and 2016 data could be the type of sampler used. Another possible explanation for these differences could be influence from filter material. The nature of the fog/rain (EC) sampler contributes towards longer possible interaction times over greater surface area, as opposed to the rain (VW) sampler where samples have lower interaction periods due to the depositional nature of the sampler.

Figures 5-1 and 5-2 present further comparisons of the sampler data, with Figure 5-1 showing differences between both samplers for the 2016 campaign, and Figure 5-2 showing differences between the same sampler over both 2014 and 2016 years. While there are clear differences present between the fog/rain sampler (EC) and the rain sampler (VW) in 2016 (average difference in freezing temperature of ~3-5 ^{o}C), Figure 5-2 shows less uniform distribution with samples from the same device compared between both 2014 and 2016. With the lack of urban

populations nearby, the wide distributions exhibited in 2014 and 2016 could be more characteristic of specific aerosol sources relative to the Arctic. With the relatively pristine nature of the Arctic atmosphere, the likely explanation for the variability seen in the Arctic samples could result from an inhomogeneous INP population within the atmospheric environment.

5.4 Alberta Sampling Observations

The precipitation data from both rural (Kananaskis) and urban (Calgary) displayed warmer freezing temperatures on average, as compared to the Arctic data from 2014 and 2016. Within those sets, the Kananaskis data exhibited freezing temperatures between ~-15 and -17 ^{o}C, while the Calgary data was ~ -18 ^{o}C.

The highest concentration of INPs was noted on June 23rd (2017) for a Kananaskis rain sample was ~ 4.5x10^{6} L^{-1}, approximately 1x10^{6} more L^{-1} than the bulk of the samples. An interesting feature in the Calgary set was the division between the bulk of the summer samples (June) and the bulk of the winter samples (Jan/Feb). Similar clumping was observed in the Kananaskis data, with notable grouping occurring between snow and rain samples, with the latter presenting clearly warmer ice nucleation temperatures. There were two exceptions to this pattern, with Feb 22nd and May 24th snow samples landing in the clustering observed for all the rain samples.

The snow samples from Feb 22nd and May 24th could have been influenced by an external Arctic or marine air mass, shifting the ice nucleating characteristics. Arctic and marine air mass back trajectories were not evident from HYSPLIT analysis in Figures 4-13, 4-14, and 4-

15. Therefore, regional continental air masses, which are dominant in Figures 4-13 through 4-15 have differences that could influence the ice nucleation characteristics.

5.5 Arctic versus Alberta

All the ice nucleation trials for Kananaskis, Calgary, and Arctic (2014 and 2016) fell within 10^4 and 10^7 ice nucleating particles L^{-1}, with freezing temperatures bound between -5 ^oC and -30 ^oC. Similar concentrations of INP's were present in all samples, with a bulk concentration falling between 10^5 and 10^6 L^{-1}. INP concentrations for bulk and microlayer seawater samples from several studies (Irish, 2018; Schnell, 1975; Vali, 2008) in both the Arctic and Atlantic were also bounded by this range. Across the suite of samples, regional differences were present (Figure 5-3). The Arctic 2014 samples presented clearly lower freezing temperatures from -18 ^oC to -28 ^oC, whereas the 2016 samples from the same region yielded a relatively evenly distribution of freezing temperatures, spanning from -11 ^oC to -29 ^oC.

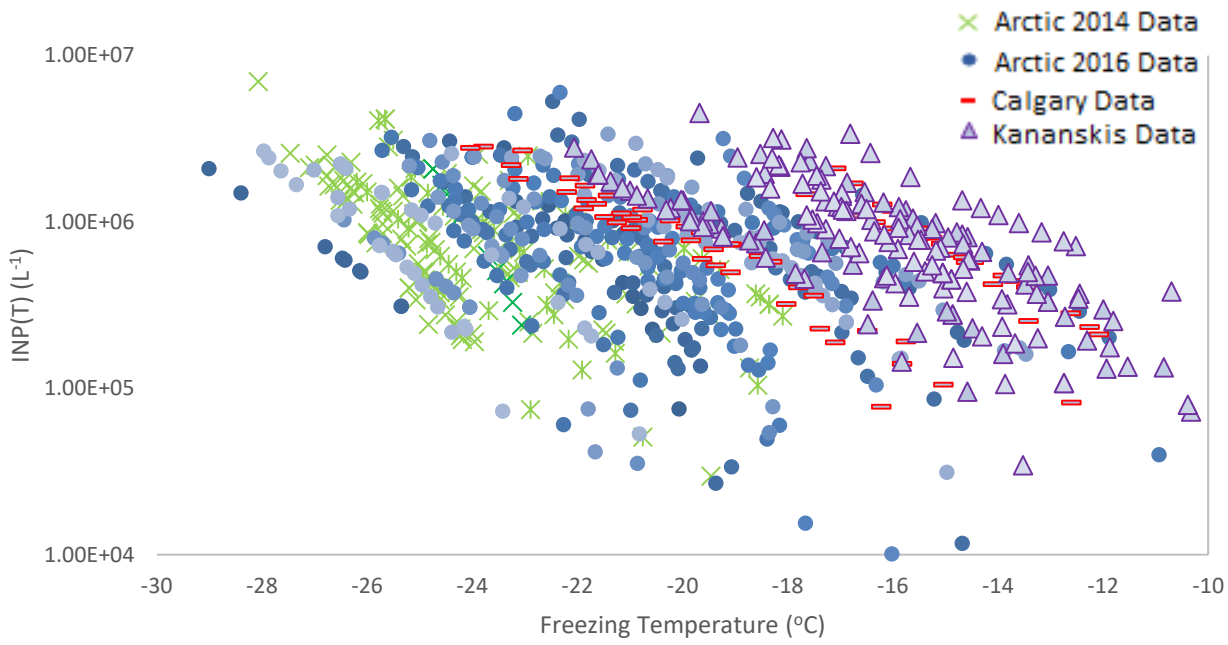

Figure 5-3 Comparison of all ice nucleation data taken during this study. Arctic 2014 data (green x), Arctic 2016 (blue circle), Calgary (red line), and Kananaskis (Purple Triangle).

5.6 Sulfur Isotopes

The δ^{34} S values versus the percentage of sea salt sulfate for the Calgary and Kananaskis is shown in Figure 5-4a. The end member assignment of +13‰ (well mixed air from oil and gas and vehicle exhaust) and +5‰ (car exhaust) dictated the mixing lines which contained all but one sample. The sample outside the dashed mixing line shown in Figure 5-4a, which is more consistent with lithospheric and/or continental biogenic sulfate (-5 ‰). There is grouping within the data below 10% sea salt sulfate, and most of the data lies along the sea salt/anthropogenic mixing line. For the Arctic samples shown in Figure 5-4b there is clear agreement with δ^{34}S values for DMS (+18 ‰), with 30% and 75% sea salt sulfate contributions. Although limited, the isotope data and end-member assignment in Figure 5-4b are consistent with previous Arctic aerosol data (Ghahremaininezhad, 2017).

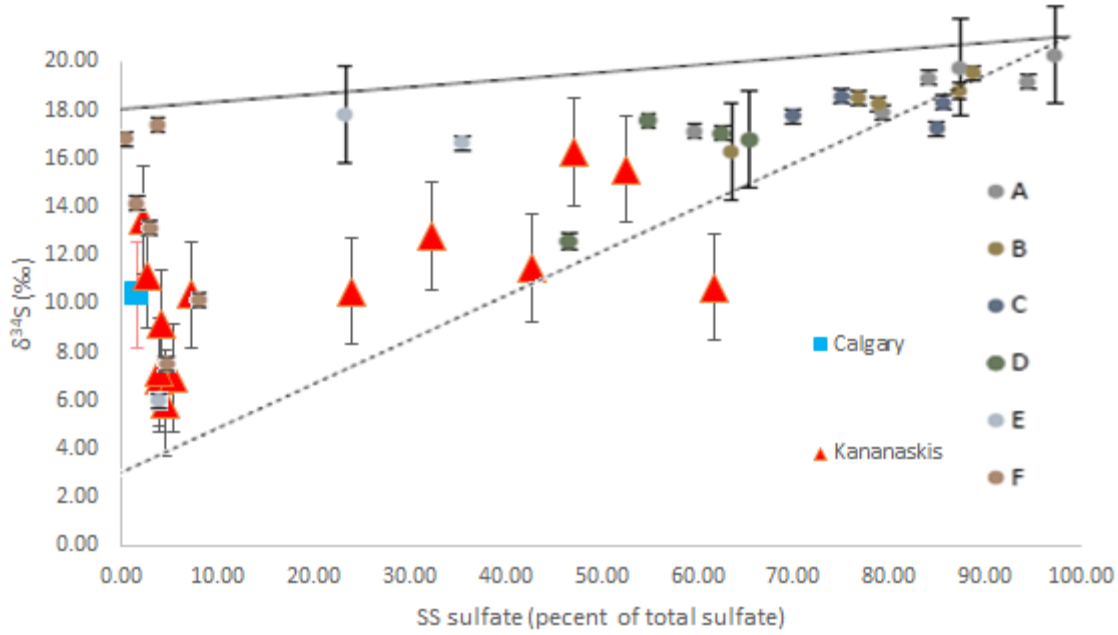

a)

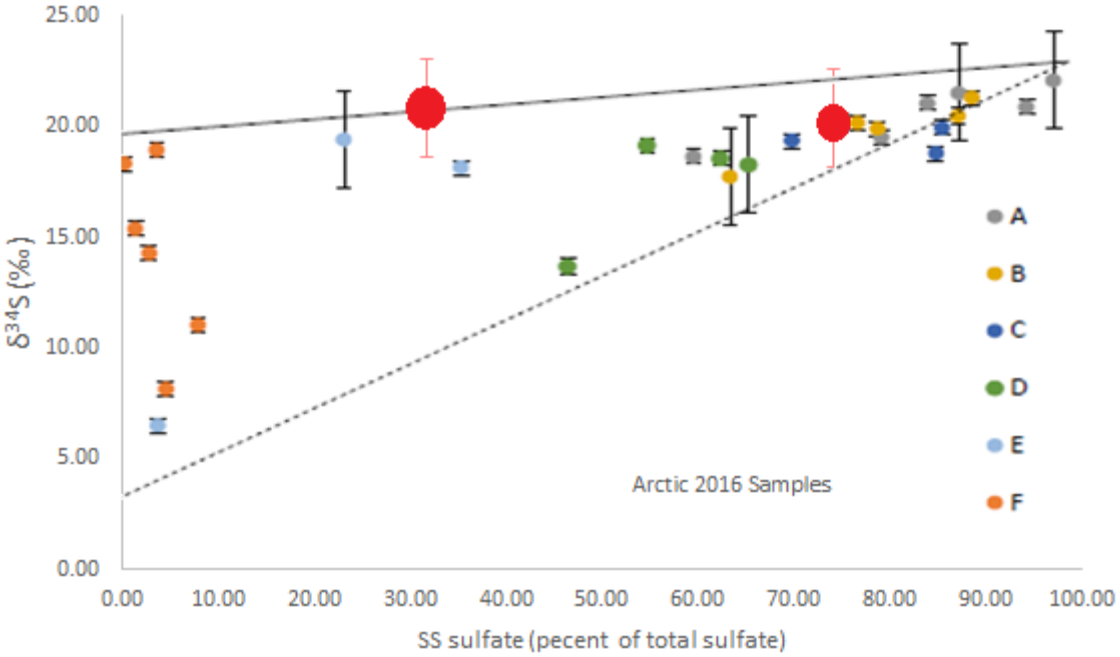

b)

Figure 5-4 Urban and rural continental sulfate (a). Comparisons of sulfur isotope values with size segregated aerosol results with Arctic samples (b). Size ranges shown are: A >7.20 µm, B 3.00-7,20 µm, C 1.50-3.00 µm, D 0.95-1.50 µm, E 0.49- 0.95 µm, and F <0.49 µm (aerosol data from Ghahremaininezhad, 2017).

5.7 Ice Nucleation Characteristics

5.7.1 Ice Nucleation Curves

In Chapter 4, the relationships between INP(T) concentrations and freezing temperatures suggested there may be differences between sample groupings (Sampler type, year, and type of sample) as a result of variations in the slopes. It has been established that for warmer freezing temperatures (~ -10 ^{o}C to -20 ^{o}C), biological particles provide more active sites of ice nucleation than anthropogenic or mineral dust sources (Atkinson et al., 2013; Prenni et al., 2009). Samples which freeze at warmer temperatures typically are associated with shallower slopes, as displayed in Figures 4-9,4-10, and 4-11. Further studies on European Arctic ice cores have also linked marine biogenic activity with both shallower slopes, and warmer freezing temperatures (Hartman et al., 2019). As a result, the slopes from the ice nucleation experiments were analyzed (Figure 5-5). The slopes from the sample groupings showed variability, with both the rural and urban continental samples possessing shallower slopes (-0.4230±0.117 in rural continental; -0.480±0.129 in urban continental). The snow and rain from Calgary and Kananaskis had similar ranges, where the dry deposition samples from the Kananaskis region had clearly steeper slopes (Appendix). The samples from the Arctic contained more variability and had distinctly steeper slopes than the samples from the urban and rural continental samples. The largest differences appeared to be present between the 2014 and 2016 fog and rain/fog samples. Between the two years of Arctic sampling, the 2014 slopes were steeper than their 2016 counterparts. With some observational differences present, statistical testing was employed to confirm any significant differences between sample groupings.

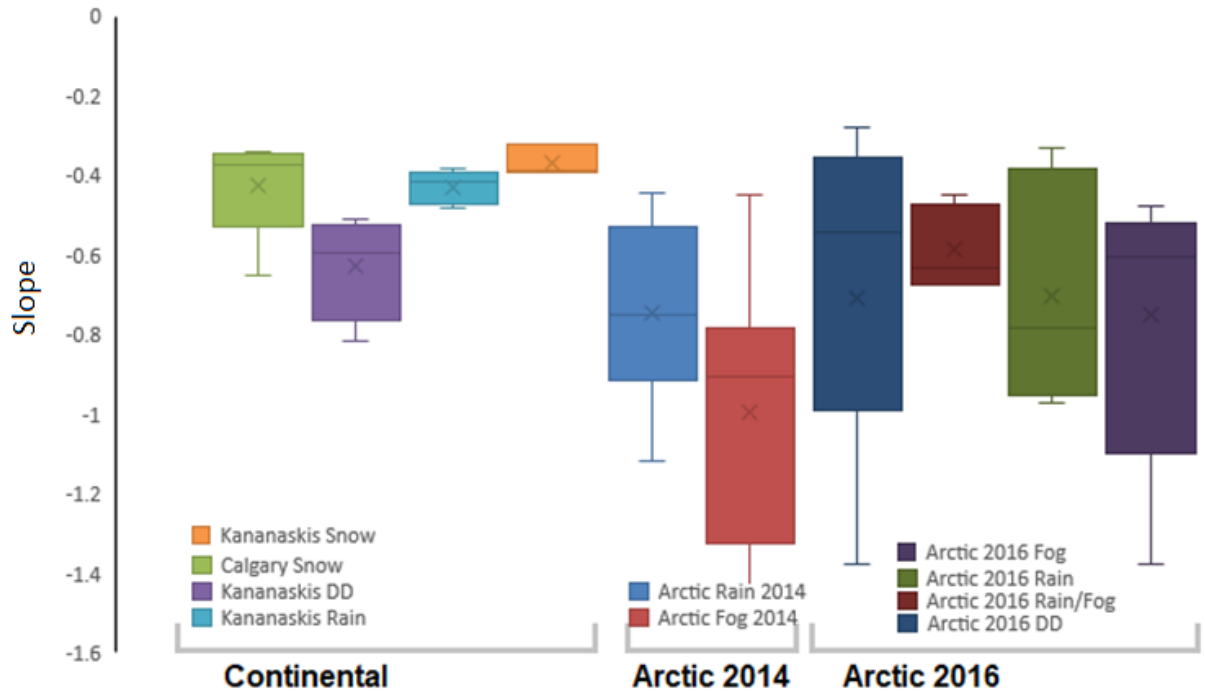

Figure 5-5 Boxplots for slopes (INP $L^{-1}T^{-1}$) representing the relationship between INP concentration and freezing point. Average values are shown with an x, and the median value is marked with a line.

5.7.2 Arctic Rain, Fog, and Dry Deposition

With observational differences present between different samplers and types of precipitation (fog, rain, dry deposition), it was important to understand whether any of these differences could significantly influence ice nucleation characteristics. In order to test for the differences in the slopes of the ice nucleation curves, the different sample characteristics were binned and tested against each other for significant differences.

The 2016 data contained categorized data (rain, fog, dry deposition) from both the passive fog/rain sampler (EC) and passive deposition-based sampler (VW). With some observational data

suggesting potential diffferences between the sampling methodology, it was neccesary to statistically test these observations. The 2016 data contained no significant difference between the two different sampling mechanisms (EC and VW) for dry deposition samples, fog samples, or rain samples. Additionally, tests using only the sampler type as the bin failed to show significant differences between the two samplers (Table 5-2). As a result, it was confirmed that there was no sampler bias towards ice nucleation characteristics.

The 2016 data contained samples from rain, fog, and mixed rain/fog events. As a result, it was nessecary to see if the mixed events were significantly different from isolated, singular precipitation events. T-tests between fog/rain + fog samples, and fog/rain + rain samples yeilded no signifficant differences (Table 5-2). With no significant differences present between the singular vs mixed event samples, the rain/fog and rain were included in the respective rain and fog catagories. Finally the dry deposition, fog, and rain samples did not reveal any significant differences between each other. The 2014 Arctic samples contained only rain and fog samples from an EC sampler, and did not reveal any significant differences between the two.

Biological activity in the Arctic is elevated as a result of increased solar radiation, exposed ocean, and sea surface temperatures (Abbatt et al., 2018). With more favorable conditions for algae production, it was suspected that the 2016 samples might present greater marine biogenic influence than the 2014 counterparts. On average, 2016 slopes (-0.675 ± 0.31) were found to be ~32% different from 2014 slopes (-0.934 ± 0.31) (Table 5-2). A t-test of the total datasets from 2014 and 2016 (rain, fog, dry deposition) produced a p-value = 0.048 (one-tailed), indicating that the two data-sets possesed significantly different ice nucleating characteristics over the two year gap. With the increased production of biogenic aerosols at a roughly 30% decade^{-1}, and the large inter-annual

changes associated with variable ice retreat, it is likely that biogenic material has greater potenital to influence ice nucleationg characteristics in the Arctic (Abbat et al., 2018).

As Table 5-2 shows, a significant difference was found between the 2014 and 2016 data. Due to this change in the ice nucleating characteristics, it was critical to understand whether these changes were more prevalent in a specific sample groupings (i.e. differences driven by rain or fog). Ice nucleating particles can be present in both fog and rain particles, but rain samples are more associated with washout of ice nucleating particles. With no differences found between groupings of the same year, similar bins from 2014 and 2016 were compared. Differences in a category (i.e. 2014 vs. 2016 rain) could indicate significant drivers in the Arctic ice nucleating process. In a one-tailed t-test, rain samples from 2014 to 2016 did not meet the 95% confindence limit (p-value=0.212). However, similar testing for 2014 vs 2016 fog samples resulted in p-value=0.036. Unfortunatly, differences between dry deposition samples were unable to be analysed, with only fog and rain data available for the 2014 voyage. The differences in fog samples was consistent with the washout of ice nucleating particles which rain samples exhibit. Therefore, the marine biogenic component of fog ice nuclei appears to be particularily relevant. A greater influence of marine biogenic ice nucleating particles is exhibited in these differences between 2014 and 2016 Arctic data, and it would appear that future studies focusing on fog charactarisitcs of ice nucleation will be highly relevant.

Table 5-2 Significant differences above the 95% confidence level found within slope differences of INP(T) concentrations vs freezing temperatures.

	P-Value (one tailed)
Kananaskis Snow vs rain	0.047
Kananaskis Rain vs Dry Deposition	0.025
Kananaskis Snow Vs Dry Deposition	0.011
Kananaskis Dry Deposition vs Calgary Snow	0.049
Rain (Arctic 2016 vs Kan)	0.029
Rain (Arctic 2014 vs Kan)	0.010
Fog (Arctic 2014 vs 2016 (Fog+Rain/Fog))	0.036
TOTAL Arctic 2014 vs Arctic 2016	0.048
Arctic Rain 2014 vs Calgary snow	0.010
Arctic Rain 2016 vs Calgary snow	0.012

5.7.3 Contrasts in Urban/Rural Continental Samples

While Arctic samples from 2014 and 2016 showed a great deal of overlap in terms of the similar ice nucleationg charactarisitcs (Figure 5-5), fluctuations in Kananaskis and Calgary data apeared to not contain as many similarities. Within the rural continental (Kananaskis) samples, it was predicted that the washout effect would again present differences between the rain and dry deposition samples, and possibly even throughout snow/dry deposition comparisons. As predicted, the Kananaskis snow and dry deposition were different (p-value = 0.011). Additionally, the differences between rain and dry deposition samples were also above the 95% confidence level (p-value = 0.025). The hypothsised washout of ice nucleating particles seemed evident in both rain and snow samples and motivated questioning whether these effects could be significantly different between rain and snow samples. Differences between Kananaskis snow and rain were significant (p-value =0.047) indicating the washout effects were potentially greater in the rain samples than the snow samples. Since differences were present between Kananaskis dry deposition and snow (Table 5-2), and Kananaskis and Calgary are within close proximity (~100 km apart), it was also

expected that the dry deposition from Kananaskis would display significant differnces with Calgary snow samples. These differences were confirmed with confidence above the 95% limit (p-value = 0.049). As seen in Figure 5-5, the slopes from the urban/rural continental samples were (from shallowest to steepest) Kananaskis snow, Calgary snow, Kananaskis rain, and Kananaskis dry deposition. The limited number of samples within each group precludes an in-depth interpretation, although it is possible that biogenic and/or non-biogenic organic materials are responsible for the shallower slopes.

5.7.4 Comparison of Continental with Arctic INP

While the critical driver of ice nucleating characteristics in the Arctic was fog based biogenic material, the comparisons of Arctic data to urban and rural continental data was limited to Kananskis rain samples, as there were no snow samples during the Arctic summers in 2014 and 2016. Comparisons of both the 2014 and 2016 Arctic rain samples with Kananasksi rain samples yeilded significant differences above the 95% confindence level (respective p-value: 0.010 ; 0.029). Differences in ice nucleating characteristics between the rural continental samples and the Arctic datasets indicate influences from regional sources, as seen in the variations in each respective study sites slopes (Figure 5-3). Larger research campaigns have suggested that Arctic aerosols are under growing influence of marine biogenic sources (Abbat et al., 2018). Additionally, it has been suggested that regional biogenic sources may be present in other enviornments (Abbat et al., 2018). While limiited, the isotopic signatures in Figure 5-4a are possibly the result of regional biogenic precursors found in urban and rural continental sample sites. The differences in ice nucleation slopes (Figure 5-3) are possibly resultant of a local biogenic or organic source.

Future studies investigating a possible continental biogenic or organic source would be a highly relevant avenue of research.

Chapter Six: Summary and Recommendations

6.1 Summary

This is the first study which combines sulfur isotopic signatures with data from ice nucleation trials for Arctic as well as urban and rural continental regions within Alberta. The results showed the important influence of marine biogenic particles in the Arctic and non-marine biogenic and/or organic material at the mid-latitude continental locations. This study showed:

1. Characteristics associated with the slope of INP versus T could be used to differentiate sample groups. Previous research demonstrated a stronger biogenic influence when slopes were shallow, so it is possible to distinguish relative proportions of biogenic influence based on the slopes from INP vs T plots.
2. Statistical differences in slopes suggest the proportion of biogenic matter contributing to INP is larger in fog than in rain and/or dry deposition in the Arctic.
3. Marine biological material influenced Arctic summertime ice nucleation characteristics to a greater extent in 2016 than in 2014. This is an important result considering the notable changes in sea ice cover and temperature in the Arctic summer as it has the potential to alter the radiation budget through precipitation type and albedo.
4. Rural and urban continental sample groupings displayed significantly different ice nucleation characteristics. These differences indicate a greater (continental) biogenic and/or organic influence in Calgary than Kananaskis.
5. Ice nucleation characteristics were not affected by sampler bias. Samples from a passive rain sampler and fog/rain sampler showed no significant differences.

The results here will be discussed in terms of the objectives laid out in Chapter 2:

> Objectives one and two were to identify the influence of sulfate in the ice nucleation process in the Arctic and both rural (Kananaskis) and urban (Calgary) continental study sites and investigate connections between sulfate sources and the study sites.

Source apportionment using sulfur isotopic analysis revealed the contributing sulfur sources to the ice nucleating particles within the precipitation samples at the different study sites. The Arctic samples were consistent with source influences from sea salt and biogenic sources, as well as sea salt and anthropogenic sulfate sources. Kananaskis (Continental Rural) samples were consistent with influence from anthropogenic sources, as well as a sea salt signature consistent with road salt. Evidence suggesting the influence of lithospheric and/or continental biogenic sulfate in Kananaskis was also present. These results indicate that sulfate is an important factor in ice nucleation processes in Arctic and rural and urban continental sites. Furthermore, distinct regional differences between local sulfate sources were seen between Arctic and continental sites, with a similar sea salt isotopic signature in both regions. Based on the isotopic data collected, there did not appear to be unexplained sources of sulfate in the samples. However, the low levels of sulfate collected in samples prevented the exploration of the linkages between ice nucleating processes and different sulfate sources, leading to a greater focus on objective three.

> Objective three was to explore the linkage between biogenic sulfate and changes in ice nucleation characteristics.

Ice nucleating particle concentrations ranged between $1x10^4$ and $1x10^7$ (L^{-1}), with no samples containing any significantly greater populations of ice nucleating particles. However, the

freezing temperature ranges for the specific sample sites differed (Figure 5-3), which suggested different levels of biological/organic matter influencing the ice nucleation characteristics. This was confirmed when the slopes of the INP(T) concentration plots were tested for significance. No variability between the ice nucleation characteristics of the 2014 and 2016 Arctic data sets was predicted at the start of this study. However, upon further analysis, differences between the 2014 and 2016 data were present, with the 2016 data presenting clearly shallower slopes. This change in the ice nucleation characteristics likely indicates an increased influence due to marine biogenic material. Given the recent trends in Arctic ice melt and rapid warming this suggests subsequent studies on precipitation and fog ice nucleation characteristics might be expected to display even shallower slopes in the future, with the anticipated increase of biological production in melt ponds and Arctic surface water (Gourdal et al., 2018).

6.2 Recommendations for Future Works

This study explored the influence of sulfate on ice nucleation characteristics and combined isotopic data with ice nucleation data for the first time. There are many opportunities for future work. Limitations which affected the study and recommendations for future avenues of research are presented as following.

1. Arctic samples possessed very low levels of sulfate which limited the extent of the sulfur isotopic analysis in our sample suite. Future work should consider pooling samples in addition to collecting larger amounts of precipitation in order to maximize concentrations of sulfate which can be used for isotopic analysis. Alternately, improved IRMS resolution for sulfur isotope measurements (< 10 mg Sulfur / sample) could resolve issues of insufficient material for isotopic analysis

of ultraclean Arctic samples. Previous isotopic source characterization studies in rural and urban continental regions have pooled samples when sulfate levels were low.

2. Processing time for ice nucleation data required significant time commitments, which limited the number of samples which were able to be studied within the scope of this project. For future studies, a beneficial addition to the ice nucleation experiments would be software developed for identification of when particles freeze. Such an addition would increase the number of data and add power to statistical analysis.
3. With the unexpected differences that came from the Kananaskis region data, further studies into the effectiveness of biological versus lithogenic influences in different types of precipitation samples could be beneficial to better understanding sulfate influences on ice nucleation. Longer-term studies could uncover explanations of any seasonal trends between the ice nucleation characteristics from dry deposition, rain, and snow samples.
4. The blanks which were taken to study the baseline of the ice nucleation characteristics in the Arctic samples were limited to a single day measurement. For the scope of a multi-year project which seeks to explain ice nucleating characteristics in the Arctic, blanks should be taken more frequently.

References

Aagaard, K., and Carmack, E. C. (1989). The role of sea ice and other fresh water in the Arctic circulation. *Journal of Geophysical Research: Oceans*, 94(C10), 14485-14498.

Abbatt, J. P. (2003). Interactions of atmospheric trace gases with ice surfaces: Adsorption and reaction. *Chemical reviews*, 103(12), 4783-4800.

Abbatt, J.P., Leaitch, W.R., Aliabadi, A.A., Bertram, A.K., Blanchet, J.P., Boivin-Rioux, A., Bozem, H., Burkart, J., Chang, R.Y., Charette, J. and Chaubey, J.P. (2018). New insights into aerosol and climate in the Arctic. *Atmospheric Chemistry and Physics Discussions*, in-press.

Alizadeh, A., Yamada, M., Li, R., Shang, W., Otta, S., Zhong, S., Ge, L., Dhinojwala, A., Conway, K.R., Bahadur, V. and Vinciquerra, A.J. (2012). Dynamics of ice nucleation on water repellent surfaces. *Langmuir*, 28(6), 3180-3186.

Almeida, J., Schobesberger, S., Kürten, A., Ortega, I.K., Kupiainen-Määttä, O., Praplan, A.P., Adamov, A., Amorim, A., Bianchi, F., Breitenlechner, M. and David, A. Molecular understanding of sulphuric acid-amine particle nucleation in the atmosphere. *Nature* 502, 359–363,

Arrigo, K. R. and G. L. van Dijken Continued increases in Arctic Ocean primary production. *Prog. Oceanogr*. 136, 60–70, (2015).

Atkinson, J.D., Murray, B.J., Woodhouse, M.T., Whale, T.F., Baustian, K.J., Carslaw, K.S., Dobbie, S., O'sullivan, D. and Malkin, T.L. (2013). The importance of feldspar for ice nucleation by mineral dust in mixed-phase clouds. *Nature*, 498(7454), 355.

Augustin-Bauditz, S., Wex, H., Kanter, S., Ebert, M., Niedermeier, D., Stolz, F., Prager, A. and Stratmann, F. (2014). The immersion mode ice nucleation behavior of mineral dusts: A comparison of different pure and surface modified dusts. *Geophysical Research Letters*, 41(20), 7375-7382.

Becagli, S., Lazzara, L., Marchese, C., Dayan, U., Ascanius, S.E., Cacciani, M., Caiazzo, L., Di Biagio, C., Di Iorio, T., Di Sarra, A. and Eriksen, P. (2016). Relationships linking primary production, sea ice melting, and biogenic aerosol in the Arctic. *Atmospheric environment*, 136, 1-15.

Bony, S., Colman, R., Kattsov, V.M., Allan, R.P., Bretherton, C.S., Dufresne, J.L., Hall, A., Hallegatte, S., Holland, M.M., Ingram, W. and Randall, D.A. (2006). How well do we understand and evaluate climate change feedback processes? *Journal of Climate*, 19(15), 3445-3482.

Breider, T.J., Mickley, L.J., Jacob, D.J., Ge, C., Wang, J., Payer Sulprizio, M., Croft, B., Ridley, D.A., McConnell, J.R., Sharma, S. and Husain, L. (2017). Multidecadal trends in aerosol radiative forcing over the Arctic: Contribution of changes in anthropogenic aerosol to Arctic warming since 1980. *Journal of Geophysical Research: Atmospheres,* 122(6), 3573-3594.

Brimblecombe, P. (2013). The global sulfur cycle. In *Treatise on Geochemistry: Second Edition* (pp. 559-591). Elsevier Inc..

Calhoun, J. A., Bates, T. S., and Charlson, R. J. (1991). Sulfur isotope measurements of submicrometer sulfate aerosol particles over the Pacific Ocean. *Geophysical Research Letters*, 18(10), 1877-1880.

Campbell, J. M., Meldrum, F. C., and Christenson, H. K. (2017). Observing the formation of ice and organic crystals in active sites. *Proceedings of the National Academy of Sciences*, 114(5), 810-815.

Charlson, R. J., Lovelock, J. E., Andreae, M. O., and Warren, S. G. (1987). Oceanic phytoplankton, atmospheric sulphur, cloud albedo and climate. *nature*, 326(6114), 655.

Chen, Y., Wang, H., Singh, B., Ma, P. L., Rasch, P. J., & Bond, T. C. (2018). Investigating the linear dependence of direct and indirect radiative forcing on emission of carbonaceous aerosols in a global climate model. *Journal of Geophysical Research: Atmospheres*, *123*(3), 1657-1672.

Croft, B., Martin, R. V., Leaitch, W. R., Tunved, P., Breider, T. J., D'Andrea, S. D., and Pierce, J. R. (2016). Processes controlling the annual cycle of Arctic aerosol number and size distributions. *Atmospheric Chemistry and Physics*, 16(6), 3665-3682.

Curry, J. A., Meyer, F. G., Radke, L. F., Brock, C. A., and Ebert, E. E. (1990). Occurrence and characteristics of lower tropospheric ice crystals in the Arctic. *International journal of climatology*, 10(7), 749-764.

DeMott, P.J., Sassen, K., Poellot, M.R., Baumgardner, D., Rogers, D.C., Brooks, S.D., Prenni, A.J. and Kreidenweis, S.M. (2003). African dust aerosols as atmospheric ice nuclei. *Geophysical Research Letters*, 30(14).

Diehl, K., Simmel, M., & Wurzler, S. (2006). Numerical sensitivity studies on the impact of aerosol properties and drop freezing modes on the glaciation, microphysics, and dynamics of clouds. *Journal of Geophysical Research: Atmospheres*, *111*(D7).

Döscher, R., Vihma, T. and Maksimovich, E (2014). Recent advances in understanding the Arctic climate system state and change from a sea ice perspective: a review. *Atmospheric Chemistry and Physics*. 14

Eastwood, M. L., Cremel, S., Wheeler, M., Murray, B. J., Girard, E., and Bertram, A. K. (2009). Effects of sulfuric acid and ammonium sulfate coatings on the ice nucleation properties of kaolinite particles. *Geophysical Research Letters*, 36(2).

Ebert, E. E., and Curry, J. A. (1992). A parameterization of ice cloud optical properties for climate models. *Journal of Geophysical Research: Atmospheres*, 97(D4), 3831-3836.

Feldl, N., Anderson, B. T., and Bordoni, S. (2017). Atmospheric eddies mediate lapse rate feedback and Arctic amplification. *Journal of Climate*, 30(22), 9213-9224.

Fridlind, A. M., and Ackerman, A. S. (2018). Simulations of Arctic Mixed-Phase Boundary Layer Clouds: Advances in Understanding and Outstanding Questions. *In Mixed-Phase Clouds* (pp. 153-183).

Gabric, A., Matrai, P., Jones, G., and Middleton, J. (2018). The nexus between sea ice and polar emissions of marine biogenic aerosols. *Bulletin of the American Meteorological Society*, 99(1), 61-81.

Ge, C., Norman, A. L., Stenhouse, K. J., Jansens, B., & Beamish, S. (2016, December). High-volume rainfall events in Calgary, Alberta, Canada and their relationship to HYSPLIT back trajectories and chemical constituents. In *AGU Fall Meeting Abstracts*.

Ghahremaninezhad, R., Norman, A.L., Croft, B., Martin, R.V., Pierce, J.R., Burkart, J., Rempillo, O., Bozem, H., Kunkel, D., Thomas, J.L. and Aliabadi, A.A. (2017). Boundary layer and free-tropospheric dimethyl sulfide in the Arctic spring and summer. *Atmospheric Chemistry and Physics*, *17*(14), 8757-8770.

Ghahremaninezhadgharelar, R. (2017). *Study of Dimethyl sulfide, Sulfate Aerosols and Ice Nucleation Particles in the Arctic Summer* (Doctoral dissertation, University of Calgary).

Ghahremaninezhad, R., Norman, A. L., Abbatt, J. P., Levasseur, M., and Thomas, J. L. (2016). Biogenic, anthropogenic and sea salt sulfate size-segregated aerosols in the Arctic summer. *Atmospheric Chemistry and Physics*, 16(8), 5191-5202.

Gorbunov, B., Baklanov, A., Kakutkina, N., Windsor, H. L., and Toumi, R. (2001). Ice nucleation on soot particles. *Journal of Aerosol Science*, 32(2), 199-215.

Gourdal, M., Lizotte, M., Massé, G., Gosselin, M., Poulin, M., Scarratt, M., Charette, J. and Levasseur, M. (2018). Dimethyl sulfide dynamics in first-year sea ice melt ponds in the Canadian Arctic Archipelago. *Biogeosciences*, *15*(10), 3169-3188.

Gurganus, C., Kostinski, A. B., and Shaw, R. A. (2011). Fast imaging of freezing drops: No preference for nucleation at the contact line. *The Journal of Physical Chemistry Letters*, 2(12), 1449-1454.

Gurganus, C., Kostinski, A. B., and Shaw, R. A. (2013). High-speed imaging of freezing drops: Still no preference for the contact line. The Journal of Physical Chemistry C, 117(12), 6195-6200.

Gurganus, S. C., Wozniak, A. S., and Hatcher, P. G. (2015). Molecular characteristics of the water-soluble organic matter in size-fractionated aerosols collected over the North Atlantic Ocean. *Marine Chemistry*, 170, 37-48.

Hansen, J. E., Lacis, A. A., Lee, P., and Wang, W. C. (1980). Climatic effects of atmospheric aerosols. *Annals of the New York Academy of Sciences*, 338(1), 575-587.

Harrington, J. Y., and Olsson, P. Q. (2001). On the potential influence of ice nuclei on surface-forced marine stratocumulus cloud dynamics. *Journal of Geophysical Research: Atmospheres*, 106(D21), 27473-27484.

Hartmann, M., Blunier, T., Brügger, S.O., Schmale, J., Schwikowski, M., Vogel, A., Wex, H. and Stratmann, F. (2019). Variation of ice nucleating particles in the European Arctic over the last centuries. *Geophysical Research Letters*, *46*(7), 4007-4016.

Haywood, J., and Boucher, O. (2000). Estimates of the direct and indirect radiative forcing due to tropospheric aerosols: A review. *Reviews of geophysics*, 38(4), 513-543.

Herbert, R. J., Murray, B. J., Whale, T. F., Dobbie, S. J., and Atkinson, J. D. (2014). Representing time-dependent freezing behavior in immersion mode ice nucleation. *Atmospheric Chemistry and Physics*, 14(16), 8501-8520.

Hiranuma, N., Augustin-Bauditz, S., Bingemer, H., Budke, C., Curtius, J., Danielczok, A., Diehl, K., Dreischmeier, K., Ebert, M., Frank, F. and Hoffmann, N. (2015). A comprehensive laboratory study on the immersion freezing behavior of illite NX particles: a comparison of 17 ice nucleation measurement techniques. *Atmospheric Chemistry and Physics*, 15(5), 2489-2518.

Hoose, C. (2012). Interactive comment on "Heterogeneous ice nucleation on atmospheric aerosols: a review of results from laboratory experiments" by C. Hoose and O. Möhler.

Huang, J., Minnis, P., Lin, B., Wang, T., Yi, Y., Hu, Y., Sun-Mack, S. and Ayers, K. (2006). Possible influences of Asian dust aerosols on cloud properties and radiative forcing observed from MODIS and CERES. *Geophysical Research Letters*, 33(6).

Ibald-Mulli, A., Wichmann, H. E., Kreyling, W., and Peters, A. (2002). Epidemiological evidence on health effects of ultrafine particles. *Journal of Aerosol Medicine*, *15*(2), 189-201.

Ice perspective: a review. *Atmos. Chem. Phys.* 14, 13571–13600, doi:10.5194/acp-14-13571-2014 (2014).

Ignatius, K., Kristensen, T. B., Järvinen, E., Nichman, L., Fuchs, C., Gordon, H., ... and Dias, A. (2016). Heterogeneous ice nucleation of viscous secondary organic aerosol produced from ozonolysis of α-pinene. *Atmospheric Chemistry and Physics*, 16(10), 6495-6509.

Intrieri, J. M., Fairall, C. W., Shupe, M. D., Persson, P. O. G., Andreas, E. L., Guest, P. S., and Moritz, R. E. (2002). An annual cycle of Arctic surface cloud forcing at SHEBA. *Journal of Geophysical Research: Oceans*, 107(C10).

IPCC, "Intergovernmental Panel on Climate Change", Christensen, J. H. et al. in Climate Change. *The Physical Science Basis* (eds Stocker, T. F. et al.) Ch. 14, IPCC, Cambridge Univ. Press, 2013.

Irish, V. E. (2018). *Ice nucleating particles in the Canadian Arctic* (Doctoral dissertation, University of British Columbia).

Karlsson, J., and G. Svensson, 2011: The simulation of Arctic clouds and their influence on the winter surface temperature in present-day climate in the CMIP3 multi-model dataset. *Climate Dyn*., 36, 623–635, doi:10.1007/s00382-010-0758-6.

Kaufman, Y. J., Koren, I., Remer, L. A., Rosenfeld, D., and Rudich, Y. (2005). The effect of smoke, dust, and pollution aerosol on shallow cloud development over the Atlantic Ocean. *Proceedings of the National Academy of Sciences of the United States of America*, 102(32), 11207-11212.

Koivurova, T. (2017). Environmental Impact Assessment (EIA) in the Arctic. *Routledge*.

Koop, T., Luo, B., Biermann, U. M., Crutzen, P. J. and Peter, T.: Freezing of HNO3/H2SO4/H2O Solutions at Stratospheric Temperatures: Nucleation Statistics and *Experiments, J. Phys. Chem. A*, 101, 1117–1133, 1997

Korolev, A., McFarquhar, G., Field, P. R., Franklin, C., Lawson, P., Wang, Z., ... and Crosier, J. (2017). *Mixed-Phase Clouds: Progress and Challenges. Meteorological Monographs*, 58, 5-1.

Krouse, H. R., and Grinenko, V. A. (1991). *Stable isotopes: natural and anthropogenic sulphur in the environment.*

Kulkarni, G., Sanders, C., Zhang, K., Liu, X., and Zhao, C. (2014). Ice nucleation of bare and sulfuric acid-coated mineral dust particles and implication for cloud properties. *Journal of Geophysical Research: Atmospheres*, 119(16), 9993-10011.

Kulmala, M., Kontkanen, J., Junninen, H., Lehtipalo, K., Manninen, H. E., Nieminen, T., ... and Franchin, A. (2013). Direct observations of atmospheric aerosol nucleation. *Science*, 339(6122), 943-946.

Kumai, M. (1961). Snow crystals and the identification of the nuclei in the northern United States of America. *Journal of Meteorology*, 18(2), 139-150.

Lewis, N., and Curry, J. A. (2015). The implications for climate sensitivity of AR5 forcing and heat uptake estimates. *Climate dynamics*, 45(3-4), 1009-1023.

Lüönd, F., Stetzer, O., Welti, A., and Lohmann, U. (2010). Experimental study on the ice nucleation ability of size-selected kaolinite particles in the immersion mode. *Journal of Geophysical Research: Atmospheres*, 115(D14).

Lupi, L., Hudait, A., and Molinero, V. (2014). Heterogeneous nucleation of ice on carbon surfaces. *Journal of the American Chemical Society*, *136*(8), 3156-3164.

Marcolli, C. (2014). Deposition nucleation viewed as homogeneous or immersion freezing in pores and cavities. *Atmospheric Chemistry and Physics*, 14(4), 2071-2104.

Marcolli, C., Nagare, B., Welti, A., and Lohmann, U. (2016). Ice nucleation efficiency of AgI: review and new insights. *Atmospheric Chemistry and Physics*, 16(14), 8915-8937.

Maxwell, B. (1992). Arctic climate: potential for change under global warming. Arctic ecosystems in a changing climate: an ecophysiological perspective, 11-34.

Murray, B. J., O'sullivan, D., Atkinson, J. D., and Webb, M. E. (2012). Ice nucleation by particles immersed in supercooled cloud droplets. *Chemical Society Reviews*, 41(19), 6519-6554.

Niedermeier, D., Shaw, R. A., Hartmann, S., Wex, H., Clauss, T., Voigtländer, J., and Stratmann, F. (2011). Heterogeneous ice nucleation: exploring the transition from stochastic to singular freezing behavior. *Atmospheric Chemistry and Physics*, *11*(16), 8767-8775.

Norman, A. L., Krouse, H. R., and MacLeod, J. M. (2004). Apportionment of pollutant S in an urban airshed: Calgary, Canada, a case study. *In Air Pollution Modeling and Its Application XVI* (pp. 107-125). Springer, Boston, MA.

Olivier, J. G. J., Schure, K. M., and Peters, J. A. H. W. (2017). Trends in global CO2 and total greenhouse gas emissions. Summary of the 2017 Report. PBL *Netherlands Environmental Assessment Agency*. The Hague.

Orellana, M. V. et al. Marine microgels as a source of cloud condensation nuclei in the high Arctic. *Proc Natl Acad Sci* 108(33), 13612–13617 (2011).

O'sullivan, D., Murray, B. J., Malkin, T. L., Whale, T. F., Umo, N. S., Atkinson, J. D., ... and Webb, M. E. (2014). Ice nucleation by fertile soil dusts: relative importance of mineral and biogenic components. *Atmospheric Chemistry and Physics*, 14(4), 1853-1867.

Pachauri, R. K., Allen, M. R., Barros, V. R., Broome, J., Cramer, W., Christ, R., ... and Dubash, N. K. (2014). *Climate change 2014: synthesis report*. Contribution of Working Groups I, II and III to the fifth assessment report of the Intergovernmental Panel on Climate Change (p. 151). IPCC.

Patris, N., Delmas, R. J., Legrand, M., De Angelis, M., Ferron, F. A., Stièvenard, M., and Jouzel,J.: First sulfur isotope measurements in central Greenland ice cores along the preindustrial periods,*J. Geophys*. Res., 107, D000672, , 2002.

Petters, M. D., and Kreidenweis, S. M. (2007). A single parameter representation of hygroscopic growth and cloud condensation nucleus activity. *Atmospheric Chemistry and Physics*, 7(8), 1961-1971.

Prenni, A. J., Petters, M. D., Kreidenweis, S. M., Heald, C. L., Martin, S. T., Artaxo, P., ... and Pöschl, U. (2009). Relative roles of biogenic emissions and Saharan dust as ice nuclei in the Amazon basin. *Nature Geoscience*, *2*(6), 402.

Prenni, A. J., and Coauthors, 2007: Can ice-nucleating aerosols affect Arctic seasonal climate? *Bull. Amer. Meteor*. Soc., 88, 541–550

Pruppacher, H. R., and Klett, J. D. (2012). *Microphysics of Clouds and Precipitation*: Reprinted 1980. Springer Science and Business Media.

Pummer, B. G., Bauer, H., Bernardi, J., Bleicher, S., and Grothe, H. (2012). Suspendable macromolecules are responsible for ice nucleation activity of birch and conifer pollen. *Atmospheric Chemistry and Physics*, 12(5), 2541-2550.

Pummer, B. G., Budke, C., Augustin-Bauditz, S., Niedermeier, D., Felgitsch, L., Kampf, C. J., ... and Schauperl, M. (2015). Ice nucleation by water-soluble macromolecules. *Atmospheric Chemistry and Physics*, 15(8), 4077-4091.

Quinn, P. K., and Bates, T. S. (2011). The case against climate regulation via oceanic phytoplankton Sulphur emissions. *Nature*, 480(7375), 51-56.

Quinn, P. K., Bates, T. S., Baum, E., Doubleday, N., Fiore, A. M., Flanner, M., ... and Shindell, D. (2008). Short-lived pollutants in the Arctic: their climate impact and possible mitigation strategies. *Atmospheric Chemistry and Physics*, 8(6), 1723-1735.

Rangel-Alvarado, R. B., Nazarenko, Y., and Ariya, P. A. (2015). Snow-borne nanosized particles: Abundance, distribution, composition, and significance in ice nucleation processes. *Journal of Geophysical Research: Atmospheres*, *120*(22), 11-760.

Ramanathan, V., and Carmichael, G. (2008). Global and regional climate changes due to black carbon. *Nature geoscience*, 1(4), 221.

Rees, C. E., Jenkins, W. J., and Monster, J. (1978). The sulphur isotopic composition of ocean water sulfate. *Geochimica et Cosmochimica Acta*, 42(4), 377-381.

Rempillo, O., Seguin, A. M., Norman, A. L., Scarratt, M., Michaud, S., Chang, R., ... and Sharma, S. (2011). Dimethyl sulfide air-sea fluxes and biogenic sulfur as a source of new aerosols in the Arctic fall. *Journal of Geophysical Research: Atmospheres*, 116(D17).

Riebeek, H. (2010). *Global warming*: Feature articles.

Rosenfeld, D. (2006). Aerosol-cloud interactions control of earth radiation and latent heat release budgets. In *Solar Variability and Planetary Climates* (pp. 149-157). Springer, New York, NY.

Rossow, W. B., and Zhang, Y. C. (1995). Calculation of surface and top of atmosphere radiative fluxes from physical quantities based on ISCCP data sets: 2. Validation and first results. *Journal of Geophysical Research: Atmospheres*, 100(D1), 1167-1197.

Schemenauer, R. S. (1986). Acidic deposition to forests: The 1985 chemistry of high elevation fog (CHEF) project. *Atmosphere-Ocean*, *24*(4), 303-328.

Schnell, R. C., and Vali, G. (1975). Freezing nuclei in marine waters. *Tellus*, 27(3), 321-323.

Schultze, M., & Rockel, B. (2018). Direct and semi-direct effects of aerosol climatologies on long-term climate simulations over Europe. *Climate dynamics*, *50*(9-10), 3331-3354.

Stenhouse, K., Matheson, A., Ge, C., Beamish, S., Jansens, B., Norman, A.L., High volume rainfall events in Calgary, Alberta, Canada and their relationship to HYSPLIT back trajectories and chemical constituents. *AGU Fall Meeting*, San Francisco, CA, Dec. 12-16, 2016, ED31B-0885 (poster).

Stein, A. F., Draxler, R. R., Rolph, G. D., Stunder, B. J., Cohen, M. D., & Ngan, F. (2015). NOAA's HYSPLIT atmospheric transport and dispersion modeling system. Bulletin of the American Meteorological Society, 96(12), 2059-2077.

Stöckel, P., Weidinger, I. M., Baumgärtel, H., and Leisner, T. (2005). Rates of homogeneous ice nucleation in levitated H2O and D2O droplets. *The Journal of Physical Chemistry* A, 109(11), 2540-2546.

Tang, M., Cziczo, D. J., and Grassian, V. H. (2016). Interactions of water with mineral dust aerosol: water adsorption, hygroscopicity, cloud condensation, and ice nucleation. *Chemical reviews*, 116(7), 4205-4259.

Team, E. W. (2005, October 01). NOAA/ESRL Global Monitoring Division – *The NOAA Annual Greenhouse Gas Index* (AGGI). Retrieved December 11, 2018, from https://esrl.noaa.gov/gmd/aggi/aggi.html

Vali, G. (1966). Sizes of atmospheric ice nuclei. *Nature*, *212*(5060), 384.

Vali, G. (2008). Repeatability and randomness in heterogeneous freezing nucleation. *Atmospheric Chemistry and Physics*, 8(16), 5017-5031.

Vali, G., DeMott, P. J., Möhler, O., and Whale, T. F. (2015). A proposal for ice nucleation terminology. *Atmospheric Chemistry and Physics*, 15(18), 10263-10270.

Vonnegut, B. (1947). The nucleation of ice formation by silver iodide. *Journal of applied physics*, 18(7), 593-595.

Welti, A., Müller, K., Fleming, Z. L., and Stratmann, F. (2018). Concentration and variability of ice nuclei in the subtropical maritime boundary layer. *Atmospheric Chemistry and Physics*, 18(8), 5307-5320.

Wilson, T. W., Ladino, L. A., Alpert, P. A., Breckels, M. N., Brooks, I. M., Browse, J., ... & Kilthau, W. P. (2015). A marine biogenic source of atmospheric ice-nucleating particles. *Nature*, *525*(7568), 234.

Woodard, D. L., Davis, S. J., & Randerson, J. T. (2019). Economic carbon cycle feedbacks may offset additional warming from natural feedbacks. *Proceedings of the National Academy of Sciences*, *116*(3), 759-764.

Wright, T. P., Petters, M. D., Hader, J. D., Morton, T., and Holder, A. L. (2013). Minimal cooling rate dependence of ice nuclei activity in the immersion mode. *Journal of Geophysical Research: Atmospheres*, *118*(18), 10-535.

Appendix

Table of slopes calculated from INP(T) data

Type	Sample Set	Sample Date	exponential fit of INP data	r^2 value of Exponential Fit	Linear slope
Rain	Arctic 2016	7/16/2019	0.0008e-0.945x	0.960	-0.945
Rain	Arctic 2016	7/19/2019	0.471e-0.826x	0.999	-0.826
Fog	Arctic 2016	7/20/2019	0.8151e-0.509x	0.996	-0.509
Fog	Arctic 2016	7/20/2019	0.955e-0.615x	0.987	-0.615
Fog	Arctic 2016	7/22/2019	212.06e^(-0.475x)	0.982	-0.475
Fog	Arctic 2016	7/23/2019	2E-07e-1.377x	0.915	-1.377
Fog	Arctic 2016	7/24/2019	8.7662e-0.594x	0.981	-0.594
Fog	Arctic 2016	7/24/2019	5.0102e-0.632x	0.861	-0.632
Fog	Arctic 2016	7/24/2019	4E-06e-1.253x	0.904	-1.253
Fog	Arctic 2016	7/24/2019	2.244e-0.556x	0.988	-0.556
Rain	Arctic 2016	8/2/2019	2013.6e-0.401x	0.991	-0.401
Rain	Arctic 2016	8/2/2019	0.021e-0.738x	0.955	-0.738
Rain	Arctic 2016	8/2/2019	4E-05e-0.973x	0.939	-0.973
Rain	Arctic 2016	8/2/2019	2002e-0.331x	0.938	-0.331
Rain/Fog	Arctic 2016	8/4/2019	0.402e-0.677x	0.922	-0.677
Rain/Fog	Arctic 2016	8/4/2019	0.3041e-0.633x	0.978	-0.633
Rain/Fog	Arctic 2016	8/11/2019	0.6715e-0.669x	0.980	-0.669
Rain/Fog	Arctic 2016	8/12/2019	31.255e-0.451x	0.947	-0.451
Rain/Fog	Arctic 2016	8/13/2019	18.041e-0.493x	0.993	-0.493
DD	Arctic 2016	7/16/2019	14.157e-0.516x	0.985	-0.516
DD	Arctic 2016	7/19/2019	0.0014e-0.989x	0.884	-0.989
DD	Arctic 2016	7/19/2019	1E-05e-1.378x	0.848	-1.378
DD	Arctic 2016	7/26/2019	0.0051e-0.917x	0.920	-0.917
DD	Arctic 2016	7/26/2019	0.0002e-0.952x	0.930	-0.952
DD	Arctic 2016	7/27/2019	1.6916e-0.505x	0.995	-0.505
DD	Arctic 2016	7/29/2019	6.1335e-0.544x	0.959	-0.544
DD	Arctic 2016	8/10/2019	5E-06e-1.077x	0.944	-1.077
DD	Arctic 2016	7/18/2019	4276e-0.281x	0.989	-0.281
DD	Arctic 2016	8/23/2019	1609.6e-0.353x	0.987	-0.353
DD	Arctic 2016	8/23/2019	1965.1e-0.291x	0.988	-0.291
Blank	Arctic 2016	8/23/2019	600.2e-0.36x	0.984	-0.360
Blank	Arctic 2016	8/23/2019	15.161e-0.58x	0.995	-0.580
Blank	Arctic 2016	8/23/2019	27.033e-0.532x	0.908	-0.532
Snow	Kananaskis	3/6/2019	2227.3e-0.323x	0.992	-0.323
Snow	Kananaskis	5/24/2019	2664.5e-0.389x	0.979	-0.389
Snow	Kananaskis	5/17/2019	464.66e-0.39x	0.974	-0.390
Rain	Kananaskis	6/23/2019	2036.4e-0.381x	0.982	-0.381
Rain	Kananaskis	6/29/2019	1819.8e-0.4x	0.954	-0.400
Rain	Kananaskis	2/9/2019	251.35e-0.418x	0.981	-0.418
Rain	Kananaskis	5/16/2019	1754.7e-0.46x	0.881	-0.460
Rain	Kananaskis	2/22/2019	551.15e-0.483x	0.985	-0.483
DD	Kananaskis	6/2/2019	207.21e-0.512x	0.989	-0.512
DD	Kananaskis	6/22/2019	101.42e-0.57x	0.978	-0.570
DD	Kananaskis	10/13/2019	19.699e-0.621x	0.979	-0.621
DD	Kananaskis	6/12/2019	1.3406e-0.815x	0.928	-0.815
Snow	Calgary	1/11/2019	34.818e-0.653x	0.955	-0.653
Snow	Calgary	1/3/2019	3875.3e-0.341x	0.988	-0.341
Snow	Calgary	1/9/2019	756.38e-0.345x	0.987	-0.345
Snow	Calgary	1/6/2019	183.19e-0.405x	0.963	-0.405
DD	Calgary	1/4/2019	530.9e-0.373x	0.977	-0.373
Fog	Arctic 2014	7/12/2019	87.923e-0.448x	0.9971	-0.448
Fog	Arctic 2014	7/17/2019	0.0063e-0.781x	0.985	-0.781
Fog	Arctic 2014	7/22/2019	0.0003e-0.847x	0.9931	-0.847
Fog	Arctic 2014	7/22/2019	7E-05e-0.908x	0.9953	-0.908
Fog	Arctic 2014	7/22/2019	2E-07e-1.218x	0.9958	-1.218
Fog	Arctic 2014	7/10/2019	(2E-08)e^(-1.323x)	0.9926	-1.323
Fog	Arctic 2014	7/17/2019	3E-10e-1.428x	0.9894	-1.428
Rain	Arctic 2014	7/20/2019	16.557e-0.442x	0.9681	-0.442
Rain	Arctic 2014	7/23/2019	4.3654e-0.56x	0.9753	-0.56
Rain	Arctic 2014	7/21/2019	0.0113e-0.769x	0.9541	-0.769
Rain	Arctic 2014	7/19/2019	0.0005e-0.848x	0.9384	-0.848
Rain	Arctic 2014	7/17/2019	0.049e-0.735x	0.8751	-0.735
Rain	Arctic 2014	7/11/2019	4E-07e-1.118x	0.9961	-1.118